Palaeogeography, Palaeoclimatology, Palaeoecology 485 (2017) 416–432

Contents lists available at ScienceDirect

Palaeogeography, Palaeoclimatology, Palaeoecology

journal homepage: www.elsevier.com/locate/palaeo

Age refinement and basin evolution of the North Rifian Corridor (Morocco): No evidence for a marine connection during the Messinian Salinity Crisis

M.A. Tulbure [a,*], W. Capella [a], N. Barhoun [b], J.A. Flores [c], F.J. Hilgen [a], W. Krijgsman [a], T. Kouwenhoven [a], F.J. Sierro [c], M.Z. Yousfi [d]

[a] Department of Earth Sciences, Utrecht University, 3584 CD Utrecht, The Netherlands
[b] Université Hassan II Mohammedia, Faculty of Science Ben M'Sik, BP7955, Morocco
[c] Department of Geology, University of Salamanca, 37008 Salamanca, Spain
[d] ONHYM, 10050 Rabat, Morocco

ARTICLE INFO

Article history:
Received 31 May 2017
Received in revised form 22 June 2017
Accepted 25 June 2017
Available online 28 June 2017

Keywords:
Mediterranean - Atlantic gateways
Planktonic foraminifera
Biostratigraphy
Paleoenvironments
Miocene

ABSTRACT

The connection between the Mediterranean and the open ocean during the Messinian and the Messinian salinity crisis (MSC) remains largely unsolved; however, such a connection is required to supply the salts required for the formation of the thick evaporite successions deposited during the MSC. A potential candidate for a Mediterranean-Atlantic connection is the northern branch of the Rifian Corridor through Morocco, but existing biostratigraphic constraints of unspecified late Tortonian – Messinian age are insufficient to test the hypothesis. We present new calcareous plankton biostratigraphic data, using among others an improved planktonic foraminiferal zonal scheme that is based on an assemblage- rather than on a typology-based taxonomic concept. The results of this study invariably reveal a late Tortonian age for the youngest open marine sediments in the individual Intramontane Basins in the central part of the North Rifian Corridor (NRC) and no marine sediments of Messinian age have been found. The high sedimentation rates and the observed shallowing in the top part of several NRC successions suggest that, although the marine connection through the NRC may have continued in the earliest Messinian, it was likely closed before ~7.0–7.2 Ma, i.e. well before the onset of the MSC. This closure is likely related to a phase of enhanced and localised uplift in the Rif foreland and excludes the North Rifian Corridor as the long-lasting marine connection between the Mediterranean and open ocean during most of the MSC.

1. Introduction

Marine gateways play a key role in thermohaline circulation and species distribution between oceans and marginal seas such as the Mediterranean. During the late Miocene, the North Rifian Corridor (NRC; Feinberg, 1986) developed as the northern and most narrow strand of the Rifian Corridor connecting the Mediterranean with the Atlantic through northern Morocco (e.g., Wernli, 1988; Achalhi et al., 2016; Fig. 1). After the closure of the Betic gateway through southern Spain (Martín et al., 2001; Martín et al., 2014), the Rifian Corridor was hypothesized to be the last marine connection with the Atlantic Ocean before the Messinian Salinity Crisis (MSC; Martín et al., 2001; Flecker et al., 2015 and references therein). During the MSC substantial amounts of primary lower gypsum precipitated (5.97–5.6 Ma) in marginal settings of the Mediterranean, followed by thick halite units (5.6–5.55 Ma) in the deep basins (Roveri et al., 2014 and references therein). Modelling studies show that although significant restriction of the seaways is required to precipitate gypsum, at least one ocean gateway must have remained open until the end of the halite stage (5.55 Ma) to supply the necessary marine waters with dissolved salts to the Mediterranean (e.g., Krijgsman and Meijer, 2008; Topper et al., 2011; Meijer, 2012; Simon and Meijer, 2015). Based on field evidence, the presence of an open MSC gateway through Morocco remains enigmatic (Krijgsman et al., 1999; Martín et al., 2001; Achalhi et al., 2016). However, based on a modelling study, the NRC could have matched the requirements for such a gateway on the grounds of width, length, and potential age (Simon and Meijer, 2015).

The uncertainty is partly due to poor age constraints on the lifespan of the NRC. Marine sediments in the corridor have been assigned an undifferentiated Tortonian–Messinian age based on foraminiferal zone m6, which ranges from 11.6 to 5.3 Ma, but does not allow a more precise age control (Flecker et al., 2015). These pioneering biostratigraphic studies (Feinberg, 1986; Wernli, 1988) do not rule out a possible connection through the NRC during the middle to late Messinian. Recently, this age was already more accurately determined for the eastern(most)

* Corresponding author.
E-mail address: m.a.tulbure@uu.nl (M.A. Tulbure).

http://dx.doi.org/10.1016/j.palaeo.2017.06.031
0031-0182/

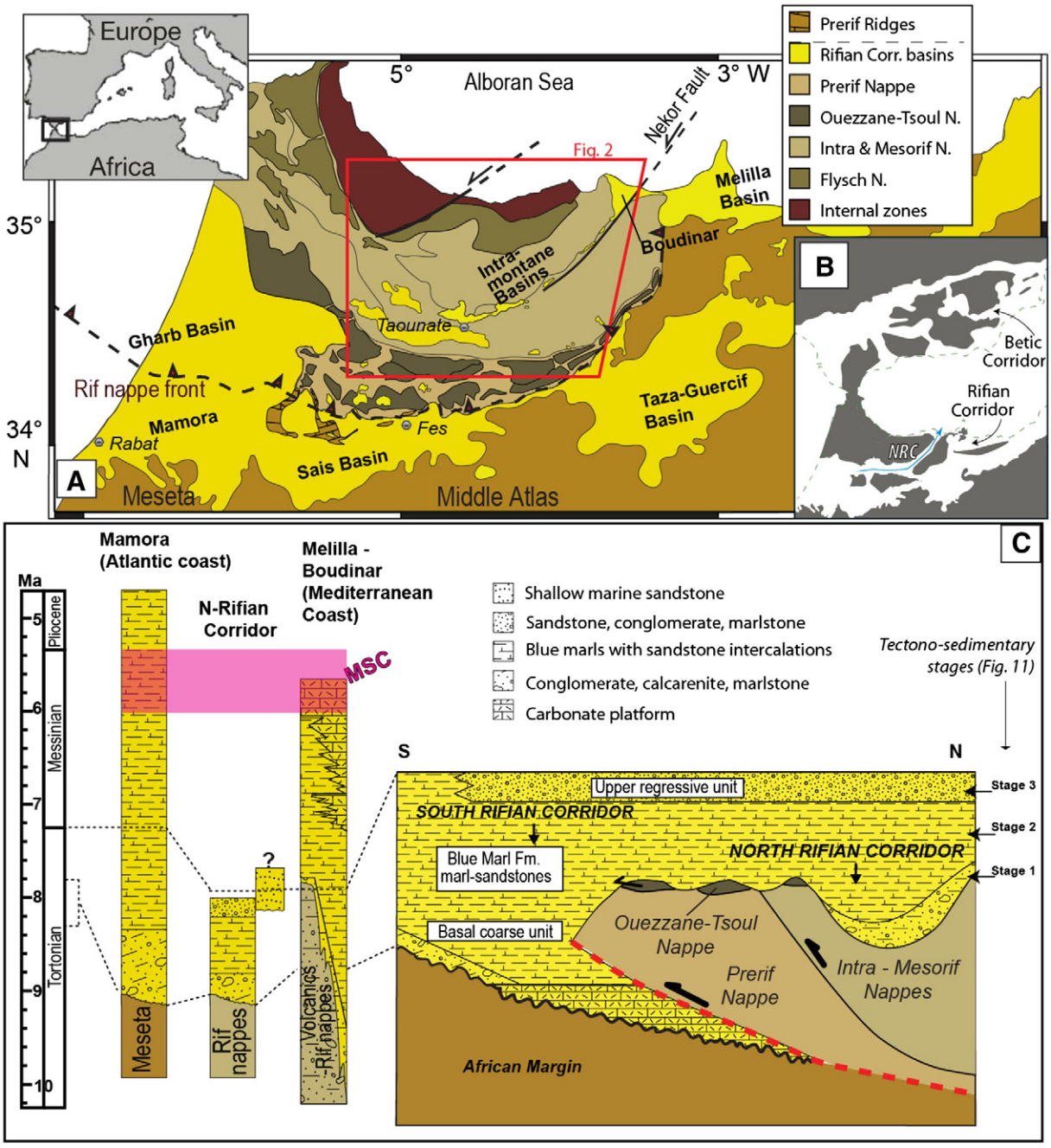

Fig. 1. A) Tectonic map of the Rif orogenic system and its foreland basins (after Wernli, 1988; Chalouan et al., 2008; Capella et al., 2017b). Red square shows the study area in Fig. 2; B) Paleogeography of the Betic-Rifian Corridors in the late Miocene. White lines are present day coastlines. After Flecker et al. (2015); C) Tectonogram and generalized stratigraphic column of three domains of the Rifian Corridor with relative correlation and relationship with the Rif foreland tectonic framework during the Tortonian and its tectono-sedimentary stages. After Van Assen et al. (2006) and Capella et al. (2017b).

part of the North Rifian Corridor, pointing to an early Messinian age for part of the sediments at Arbaa Taourirt (Achalhi et al., 2016; ~8–6 Ma). To further improve the age refinement of the NRC and to examine whether it could have been the open seaway during the peak stages of the MSC, we re-evaluated the planktonic foraminiferal biostratigraphy of the Intramontane Basins of Northern Morocco (Fig. 2), using modern biozonal schemes that have been developed for the Mediterranean and the adjacent Atlantic side (e.g. Sierro et al., 1993; Krijgsman et al., 1995; Sprovieri et al., 1999; Hilgen et al., 2000a, 2000b; Krijgsman et al., 2004). For this purpose, we analysed both new samples from the hemipelagic marls of Ghafsai, Bou Haddi, Dhar Souk, Sidi Ali Ben Doued, Boured, Arbaa Taourirt Basins (Fig. 2), as well as previously studied samples of the Intramontane Basins, collected for regional geological mapping during the 1970's and stored in the archive of the Moroccan Ministry of Geology in Rabat (Wernli, 1988). In addition, the calcareous nannofossil biostratigraphy of most of these samples was established to independently check the outcome of the planktonic foraminiferal analysis. For the Taounate Basin (Fig. 2), we also present a correlation from outcrops to a seismic section, which is then integrated with structural information (Aït Brahim and Chotin, 1989; Tejera de Leon et al., 1995; Samaka et al., 1997) to discuss basin evolution within the palaeo-seaway. We conclude that the NRC was a deep strand of the Moroccan seaway

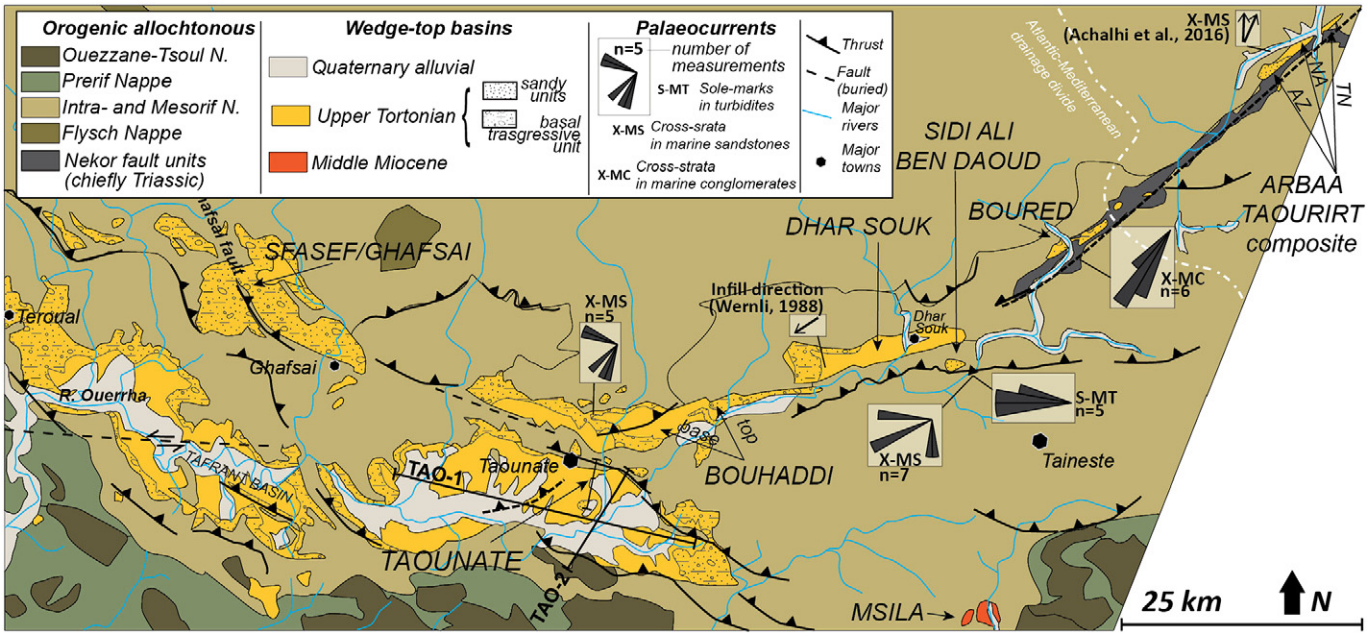

Fig. 2. Detailed geological map of the Intramontane Basins, with location of the studied sections and main fault trends (after Samaka et al., 1997; Capella et al., 2017b). Map location in Fig. 1.

during the late Tortonian, which started to be uplifted and restricted during the latest Tortonian and possibly earliest Messinian, and was probably closed before ~7.0–7.2 Ma.

2. Geological setting

2.1. Rif Mountains evolution

The NRC was a body of water that stretched across the external zones of the Rif fold and thrust belt at a time that these were mostly emplaced (Capella et al., 2017b). The Rif-Betic fold and thrust belt formed during Africa – Iberia convergence, but was driven in particular by the rapid retreat of the Gibraltar slab, associated with the extension and westward drift of the Alboran domain during Neogene times (Platt et al., 2003; Vergés and Fernàndez, 2012; Platt et al., 2013; Van Hinsbergen et al., 2014). The Alboran domain was thrusted over the external Rif fold and thrust belt during a phase of nappe stacking in Early-Middle Miocene times, and subsequently exhumed (e.g., Martínez-García et al., 2013; Romagny et al., 2014). From North to South, the fold and thrust belt is made of (i) Flysch Units that comprise turbidites deposited in the Ligurian – Maghrebian Ocean (Chalouan et al., 2008), and (ii) Intrarif, Mesorif and Prerif Units that contain deformed Mesozoic-Paleogene sediments from the rifted African margin (e.g., Wildi, 1983; Crespo-Blanc and Frizon de Lamotte, 2006). Following the last pulse of formation of the fold and thrust belt at around 8 Ma (e.g., Capella et al., 2017b), sedimentation took place in the so-called post-nappe basins (Feinberg, 1986; Wernli, 1988) comprising both the Intramontane Basins of the NRC to the north (e.g., Wernli, 1988; Aït Brahim and Chotin, 1989; Tejera de Leon et al., 1995; Samaka et al., 1997; Achalhi et al., 2016), which developed unconformably as wedge-top basins on the fold and thrust belt, and the foredeep basins to the south, forming the South Rifian Corridor (Krijgsman et al., 1999; Capella et al., 2017a; Fig. 1). In the Rif foredeep basins (i.e., Saiss and Taza-Guercif Basins), the transition from marine to molassic (continental) sedimentation is locally preserved (e.g., Krijgsman et al., 1999; Gelati et al., 2000; Sani et al., 2007). By contrast, the Intramontane Basins of the NRC usually lack the molassic unit, and open marine clastics of late Miocene age are capped by erosional unconformities (Wernli, 1988; Samaka et al., 1997; Achalhi et al., 2016).

The Intramontane Basins of the NRC are traditionally regarded as post-nappe (i.e., post-dating orogen build-up), resulting from NE-SW compression and associated orthogonal extension (Aït Brahim and Chotin, 1989; Morel, 1989). Despite the "post-nappe" designation, some of the sedimentary successions involved appear to have been deposited on top of a moving orogenic wedge and show, at least in the oldest parts, syn-kinematic features such as intraformational unconformities (Aït Brahim and Chotin, 1989; Tejera de Leon et al., 1995; Samaka et al., 1997; Capella et al., 2017b). Syn-depositional faults accommodated the deposition of thick sequences (~2000 m) of late Miocene age in the Taounate and Tafrant basins; these faults were reactivated during a late stage of uplift, which postdated nappe emplacement (Samaka et al., 1997; Capella et al., 2017b).

The sedimentary relicts of the NRC are distributed across approximately ~100 km, along the Mesorif – Intrarif boundary following a NE-SW trend (Fig. 2). This boundary is locally marked by the Nekor Fault zone (Fig. 2) (e.g., Frizon de Lamotte, 1979; Frizon de Lamotte, 1981; Guillemin and Houzay, 1982), which is sealed by Upper Miocene sediments in the Boured, Arbaa Taourirt and Boudinar areas (Wernli, 1988; Achalhi et al., 2016). This fault represented a major tear fault during the south-westward emplacement of the Rif nappes (thrust-sheets) that occurred in the early to middle Miocene, associated with the westward drift of the Alboran Domain (e.g., Frizon de Lamotte, 1981; Morel, 1989; Platt et al., 2003). Asebriy et al. (1993) proposed that strike-slip motion along the NE-SW orientated Nekor Fault continued in the late Miocene, opening the Intramontane Basins, but this hypothesis has not been substantiated by sufficient field structural data (Samaka et al., 1997).

2.2. The North Rifian Corridor

The Intramontane Basins forming the NRC comprise, from West to East, Ghafsai, Tafrant, Taounate, Bou Haddi, Dhar Souk, Sidi Ali Ben Daoud, Boured, Arbaa Taourirt, and, finally, Boudinar at the Mediterranean end of the strait (Figs. 1, 2). Individual basins contain up to 2000 m in thickness of upper Miocene sediments that unconformably overlie the previously deformed Intrarif and Mesorif units (Wernli, 1988; Tejera de Leon et al., 1995; Samaka et al., 1997; Chalouan et al., 2008).

The lithostratigraphy of the Intramontane Basins documents continuous dominantly clastic marine sedimentation unconformably deposited on top of the Rif thrust sheets (Fig. 2B). Clastic sedimentation starts with poorly sorted conglomerates, marls and calcarenites, followed by thick alternations of mud-dominated sediments (grey marl) with intercalated sandstone or fine conglomerates. The top of the marine succession is generally truncated by erosion and covered by Quaternary continental deposits (Wernli, 1988). Evidence of a shallowing trend is in general lacking, with the two following exceptions: (i) Taounate, where a continental 'molassic' facies overlies marine marls below the unconformable contact with the Plio-Quaternary (Wernli, 1988), (ii) Boudinar Basin, which as an embayment of the Mediterranean Sea and records marine sedimentation until ~6 Ma (Cornée et al., 2016; Achalhi et al., 2016), similar to the neighbouring Melilla Basin (Cunningham et al., 1997; Cornée et al., 2002; Van Assen et al., 2006).

Achalhi et al. (2016) proposed that the NRC opened in the late Tortonian and that connections with the Mediterranean Sea lasted until ~6.5–6.1 Ma. The main evidence for the Mediterranean – Atlantic connection through the NRC during the Messinian is the ~100 m thick cross-stratified unit (sands and conglomerates) that overlies the early Messinian at Arbaa Taourirt. This cross-stratified unit has been interpreted as a product of Atlantic waters flowing into the Mediterranean, and its age is based on the presence of the planktonic foraminifer *Globorotalia miotumida* and the calcareous nannofossil *Amaurolithus primus*, and the correlation of regional unconformities (Achalhi et al., 2016).

3. Methods

3.1. Planktonic foraminiferal biostratigraphy

3.1.1. Concept

To establish an improved age model for the upper Miocene successions and better date the evolution of the NRC we performed a detailed planktonic foraminiferal biostratigraphic analysis of both previously studied samples (Wernli, 1988) and new samples from key sections that were collected during field campaigns in 2013 and 2014 in the Intramontane Basins (Fig. 2).

In case of the newly collected samples, a full count of ~300 specimens from the >150 μm size fraction of the planktonic foraminiferal assemblage of the washed residue was carried out to obtain information about the abundance of marker species as percentage of the total planktonic foraminiferal fauna. In addition, a semi-quantitative analysis of the planktonic foraminiferal marker species was performed on the same size fraction to gain more insight in the morphological variation in the assemblages of the marker species and their coiling direction.

The examination of the samples from the Wernli collection focused on evaluating the trends in the marker species. We applied modern taxonomic concepts and marked the changes in coiling direction of the keeled and unkeeled globorotaliids, and of the neogloboquadrinids (see below). Notes were further made on the relative abundance of the associated *Globigerinoidess obliquus extremus* and *Sphaeroidinellopsis seminulina*.

Rather than following the typology-based taxonomic concept of planktonic foraminiferal marker species and the associated biostratigraphic scheme of Wernli (1988), previously used to biostratigraphically date sections in the NRC, we applied the high-resolution astronomically calibrated planktonic foraminiferal astrobiochronology that was initially developed by Zachariasse (1975) and elaborated by Langereis et al. (1984), Krijgsman et al. (1994, 1995, 1997, 1999, 2002) and Hilgen et al. (1995) for the Mediterranean. This chronology, which is essentially based on an assemblage-based concept of the marker species, is very similar to the chronology independently developed for the adjacent Atlantic by Sierro (1985) and Sierro et al. (1993), as far as the order of the main bio-events is concerned. Astronomical calibration of the Oued Akrech and Ain el Beida sections located on the Atlantic side of Morocco showed that these events have exactly the same age as in the Mediterranean (Hilgen et al., 2000a, 2000b; Krijgsman et al., 2004). This planktonic foraminiferal astrobiochronology was successfully applied to cores from the Guadalquivir basin in southern Spain, resulting in an improved age model for the Atlantic side of the Mediterranean in Spain (Van den Berg et al., 2016, 2017). For these reasons, we decided to apply the same astrobiochronology to our sections from the Northern Rifian Corridor. Among others, this will facilitate the identification of the Tortonian-Messinian boundary and hence distinguish between the late Tortonian and early Messinian. The ages of the selected events in the Mediterranean and adjacent Atlantic are given in Table 1.

3.1.2. Marker species and counting method

Historically, most biostratigraphic frameworks published for Neogene basins in the NE Atlantic and Mediterranean are mainly based on the occurrence of single species and do not look at the whole planktonic foraminifer assemblage. The presence of *G. miotumida*, *G. conomiozea* or *Globorotalia mediterranea* has traditionally been presented as a real proof of Messinian age, whereas the rest of the assemblage has been ignored. In the Atlantic, sediments with abundant *G. miotumida* in combination with abundant dextral forms of the *G. scitula* group can be related to the Messinian because they are younger than the sinistral to dextral coiling change of *G. scitula* (event A of Sierro et al., 1993 that occurred immediately prior to the T/M boundary). However, sediments with *G. miotumida* and *G. menardii* 4 with common sinistral forms of the *Globorotalia scitula group* (including *G. suterae*) usually occur in the late Tortonian, because during this period sinistrally-coiled *G. scitula* is very abundant.

An important criterion that is often used in our astrobiochronological framework is the abundance of marker species rather than the first or last occurrences (FO and LO, respectively) of these species. Changes in relative abundance of marker species define events where common has been added as indicator to the event label, such as Last or First Common Occurrences (LCO and FCO, respectively). The available quantitative data show that the dominantly sinistrally coiled *Globorotalia miotumida* group is found in percentages of 5–20% in sections in the Guadalquivir Basin of Spain (Sierro, 1985) and of 10–20% at Oued Akrech in Morocco (Hilgen et al., 2000a, 2000b) in the interval following the *G. miotumida* FCO that approximates the Tortonian-Messinian boundary. However, specimens of the *G. miotumida* group may already be found in low numbers during the late Tortonian, while two short influxes including larger numbers already occur around ~7.8 Ma in the Mediterranean (Krijgsman et al., 1995). The group of *G. miotumida* (including highly conical types, such as *Globorotalia conomiozea*) is present in the North Atlantic during the Late Tortonian, for example at DSDP sites 410, 397 and 334 (Sierro et al., 1993). For this reason Sierro (1985) suggested to place the Tortonian-Messinian boundary at the replacement of the group of *Globorotalia menardii* dextral (*G. menardii* 5) by the group of *G. miotumida*. Hilgen et al. (2000a, 2000b) located the boundary at the FCO of *G. miotumida*, noting that these forms were present well before the boundary. Similarly, *Globorotalia menardii* form 5 reaches percentages of 5–10% in the Guadalquivir sections and 10–15% at Oued Akrech in the interval marked by the FCO and LCO of the nominal species between 7.35 and 7.25 Ma. Again rare specimens of dextral *G. menardii* form 5 can already been found prior to 7.35 Ma. Finally, dominantly sinistrally coiled *G. menardii* form 4 reaches percentages between 10 and 15% in the Oued Akrech section (Hilgen et al., 2000a, 2000b) during its last major influx around 7.52 Ma. Both below and above the level corresponding to 7.52 Ma, *G. menardii* form 4 is often found, albeit in much lower numbers and percentages that do not exceed 1–2%.

In order to estimate the abundance of the Planktonic foraminifer marker species we performed a semiquantitative study, defining three categories: Abundant (more than15 specimens per 45squre field), common (6 to 14 specimens per 45 square field) and rare (1 to 5 specimens per 45 square field). In a full picking tray, the number of targeted marker species has been counted.

Table 1
Main bioevents used to date the Rifian Corridor sediments. References are for the astronomically calibrated ages in the Mediterranean region and its Atlantic side.

Event no.	Planktonic foraminifer bioevents	Age (Ma)	Atlantic	Mediterranean
1	Sinistral to dextral coiling change (S/D) of *Neogloboquadrina acostaensis*	6.35	Sierro et al., 1993	Hilgen and Krijgsman, 1999; Sierro et al., 2001; Lourens et al., 2004
2	Replacement of *Globorotalia menardii* 5 by *Globorotalia miotumida* group	7.25	Sierro, 1985; Sierro et al., 1993; Hilgen et al., 2000a	Sierro et al., 2001; Lourens et al., 2004
3	S/D coiling change of *Globorotalia scitula*	7.28	Sierro, 1985; Sierro et al., 1993; Hilgen et al., 2000a; Lourens et al., 2004	Sierro et al., 1993; Lourens et al., 2004
4	First common occurrence (FCO) of *G. menardii* 5	7.35	Sierro, 1985; Sierro et al., 1993; Hilgen et al., 2000a; Lourens et al., 2004	Krijgsman et al., 1995; Hilgen et al., 1995; Lourens et al., 2004
5	Last common occurrence (LCO) *Globorotalia menardii* 4	7.51	Sierro, 1985; Sierro et al., 1993; Hilgen et al., 2000a; Lourens et al., 2004	Krijgsman et al., 1995; Hilgen et al., 1995; Lourens et al., 2004
6	(Dextral to sinistral (D/S) coiling change of *G. scitula* group	7.58		Krijgsman et al., 1997; Lourens et al., 2004
7	First occurrence (FO) of *Globorotalia suterae*	7.8		Sprovieri et al., 1999
8	Lowest common occurrence (lro) of *Sphaeroidinellopsis seminulina*	7.92		Krijgsman et al., 1995; Hilgen et al., 1995; Lourens et al., 2004; Hüsing et al., 2009
9	Onset dominant sinistral Neoglobquadrinids	7.92–8 Ma		Krijgsman et al., 1995; Hilgen et al., 1995
10	FO of *Globigerinoides obliquus extremus* (Mediterranean)	8.37	Tropical Atlantic: 8.93 Ma (Lourens et al., 2004)	Sprovieri et al., 1999
11	Last occurrence (LO) of *Globorotalia lenguaensis* (Mediterranean)	~ 8.37	Tropical Atlantic: 8.97 Ma (Turco et al., 2002)	Foresi et al., 2002; F. Lirer, pers. comm.
12	Highest regular occurrence dextral(hro) *N. acostaensis*	9.51		Krijgsman et al., 1995; Hilgen et al., 1995; Lourens et al., 2004
13	FRO *N. acostaensis*	10.57		Hilgen et al., 2000a, 2000b; Lourens et al., 2004

Note that these numbers are not percentages of the marker species in the foraminifer assemblage. They are related with the concentration of these marker species in the sediment.

3.1.3. Comparison with Wernli (1988)

Wernli (1988) presented a planktonic foraminiferal zonation and compared that with existing zonations for the Mediterranean. The base of his Miocene Zone m6 was defined by the First Appearance Datum (FAD) of *Globorotalia dutertrei*; this zone was later subdivided in subzones m6a and m6b using the first appearance of *Globorotalia primitiva* (Wernli, 1977). The Miocene-Pliocene boundary was equated with the m6-P1 zonal boundary defined by the FAD of *Globorotalia margaritae*. Subzone m6a was further subdivided in m6aα and m6aβ using the *G. conomiozea* FAD, which was supposed to precede the FAD of *G. primitiva*. Wernli (1977) shows these two bio-events to be coincident in the Oued Akrech section. As a matter of fact, his *G. conomiozea* FAD is placed at the same level as in the more recent high-resolution study of Hilgen et al. (2000a, 2000b), at or close to the Messinian GSSP subsequently defined at Oued Akrech.

However, the typological species concept used by Wernli (1988) becomes less clear in other Moroccan sections if one follows this concept rather than the assemblage approach used in the present study. Rare specimens of typical *G. conomiozea* (and *G. miotumida*) found below the Messinian GSSP will in that case result in a lowering of the position of the local subzonal boundary, while these will be incorporated in the *G. menardii* form 4, if one applies the assemblage-based species concept. The same misunderstanding may arise from rare specimens of *G. menardii* form 5 encountered below the FCO of this taxon. Meanwhile, detailed integrated stratigraphic, correlations, including a high-resolution tuned cyclostratigraphy, have confirmed the time stratigraphic significance of our main bio-events founded on the assemblage-based taxonomic concept. This approach combined with the relative abundance of marker species is considered of critical importance for the success of the present study.

3.2. Calcareous nannofossils

For the study of calcareous nannofossils smear-slides have been performed. A small fraction of sediment is spread out with buffered water on a cover-slide and fixed to a glass slide with Canada balsam. The observation and identification of taxa was carried out with a petrographic microscope (×1000).

Concentration of nannoliths is variable, ranging from 5 to 200 liths per visual field (except barren samples). In all cases, at least 5 transects have been observed, assuring that each of the samples has taken into account those taxa that appear in proportions higher than 0.001% (with a probability of success of 99%) (Dennison and Hay, 1967).

For identification, Young et al. (2014) was used. For the definition and calibration of CN events, Flores and Sierro (1989) was followed, Raffi and Flores (1995) and Raffi et al. (2006), combining qualitative and semi-quantitative information.

3.3. Paleobathymetry estimates

The benthic foraminiferal assemblages from the washed fractions > 150 μm of selected samples were studied to estimate paleodepth and paleo-environment at time of deposition. Unlike the planktonic foraminifera that allow highly accurate biostratigraphy, many species of benthic foraminifera remained morphologically similar throughout the Middle-Late Miocene. Therefore, in each case we tested the planktic assemblage for possible reworking from older Miocene units. Planktonic-benthic (P/B) ratios were not considered reliable for depth estimates because most samples show signs of transport and some contain reworked specimens. Instead, semi-quantitative data of the benthic assemblages was used together with information on (differential) preservation, grain size sorting and reworking.

Depth-distributions of groups of benthic foraminifera known from literature were applied (e.g. Pérez-Asensio et al., 2012; Schönfeld, 1997; Schönfeld, 2002). Although the slope profiles of the Rifian Corridor are likely to have been different from the continental margins on which these estimates are based, inferences on the depth of the environment of deposition can be based on benthic foraminiferal assemblages and marker species with known present-day depth distribution (e.g., Capella et al., 2017a). In assemblages where both shelf- and slope-type species are present, and in absence of reworking, we considered that the shallow marine species (such as discorbids, *Ammonia*, *Elphidium* and *Rosalina* species: e.g. Rogerson et al., 2011) were transported downslope.

3.4. Seismic interpretations

The seismic profiles in the Taounate Basin (Fig. 2) were acquired by ONHYM for medium depth petroleum exploration targets. These profiles were interpreted by projecting the formation boundaries displayed on the regional geological maps (e.g., Suter, 1961; Suter and Mattauer, 1964; Suter, 1980). The Upper Miocene succession was further subdivided in unconformity-bounded depositional units. Seismic stratigraphy of tectonically active basins evolved from standard sequence stratigraphy by identifying tectonically-induced, unconformity-bounded depositional units, or 'tectonic system tracks' (e.g. Prosser, 1993). Accordingly, the depositional units in this study were characterised on the basis of internal geometry, amplitude and frequency of reflectors. The results are compared with micro-scale kinematic indicators presented in literature (Aït Brahim and Chotin, 1989; Morel, 1989; Capella et al., 2017b). Finally, the biostratigraphic results of this study were combined with the stratigraphic interpretation of the seismic profiles.

4. Results

4.1. Sfasef

4.1.1. Field observations and lithology

The Sfasef section is located in the Ghafsai Basin. At this location, upper Miocene clastics unconformably overlie the orogenic wedge (Mesorif units). The sequence is formed by alternations of mudstone and 10 to 20 m thick sandstone intervals. A panoramic view shows the progressive tilting of strata at this location (Fig. 3B). The section shows tabular massive sandstones up to 20 m in thickness, locally showing thin mud–lenses interfingered with finely–bedded sandstones (Fig. 3C).

4.1.2. Planktonic foraminiferal biostratigraphy and age

The lowermost samples of the Sfasef section contain up to 10–15% of the sinistrally coiled *G. menardii* form 4, while this percentage is lower in the upper samples. The *Globorotalia scitula* group and the neogloboquadrinids are both predominantly sinistrally coiled.

The marker species indicate a late Tortonian age between the dextral to sinistral coiling change of the *G. scitula* group at 7.58 Ma and the *G. menardii* form 5 FCO at 7.35 Ma. The higher percentages of the *G. menardii* form 4 may well correspond to the last influx of common *G. menardii* form 4 that ends with the LCO of *G. menardii* form 4 at 7.51 Ma.

4.1.3. Palaeo-bathymetry and depositional environment

Benthic assemblages are relatively diverse, containing *Cibicides pachyderma*, *Globocassidulina subglobosa*, *Uvigerina peregrina* and *P. ariminensis*, suggesting depths corresponding to outer shelf (150–300 m).

4.2. Taounate

4.2.1. Field observations and lithology

The Upper Miocene succession at Taounate developed unconformably on top of the Intra- and Mesorif Jurassic and Cretaceous units to the north and above the Ouezzane Nappe and the Prerif units to the South. Synclinal structures with the highest angles of dip in the northern margin are observed. The basal unit, only outcropping to the north and east of the basin (Tejera de Leon et al., 1995), is composed of medium to coarse bioclastic sands, locally cemented, changing upward into a detritic packstone or biocalcarenite (defined as coquinoid limestone, '*calcaire à lumachelliques*' in Wernli, 1988) intercalated with silty marls. This unit shows well-preserved autochthonous fossil content such as pectinids, bryozoans, algae, and brachiopods. The succession follows with ~100 m thick sand-marl alternations where the sand beds contain angular clasts, and can be interpreted as microconglomeratic lenses, suggesting debritic flow in marginal settings. Thin intercalations of sandbeds and marine conglomerates bear pebbles from Cretaceous units to the North. Local slump levels are present, possibly indicating tectonic instability of the nearby margin. The interbedded marls, silty and grey, contain bivalves and iron crusts. Above the sands-marl alternations the succession is composed of laterally discontinuous

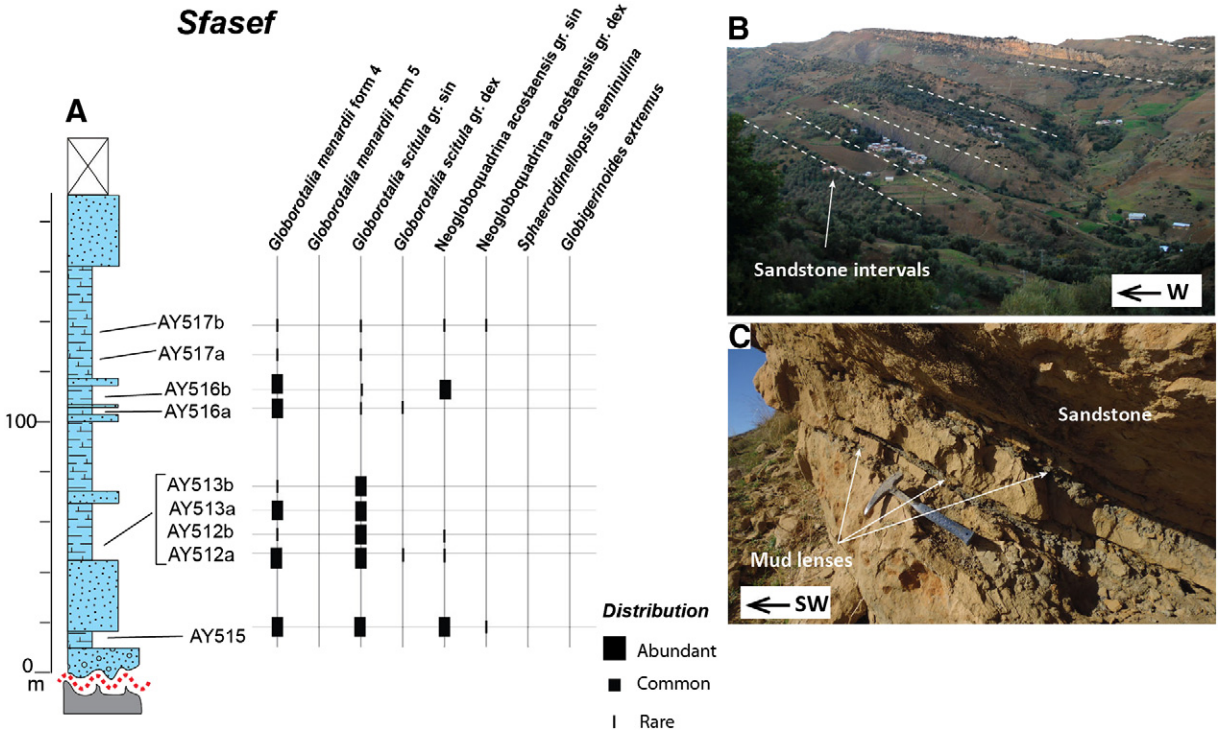

Fig. 3. Details of the Sfasef section (Ghafsai Basin): A) Sedimentological log with distribution of planktonic foraminifera and palaeoenvironmental interpretation (legend in Fig. 6). B) Panoramic view of the synkinematic wedge formed by sandstone –marlstone intervals; C) Detail of the pinching-out geometry of mud layers in the sandstone intervals.

polymictic conglomerates, reaching up to 40 m of thickness; these are very well exposed to the South of the Taounate ridge but also to the north, in the Bouhaddi Basin (Fig. 2). This conglomeratic unit, which is locally reddish and indurated but still contains shell fragments and intercalations of pelites, reflects enhanced continental input and the proximity of a river delta, possibly located near to the alluvial fans of the proto-Rif Mountains to the north. This conglomeratic unit follows with marl and sparse intercalations of sands, reaching up to ~1000 m of thickness in the centre of the Taounate Basin. At the top of the sequence is a ~30 m thick continental unit, consisting of silty muds and sandstones without microfauna.

4.2.2. Planktonic foraminiferal biostratigraphy and age

The marker species in the Taounate basin overall show a low abundance. When found, keeled globorotaliids are represented by sinistrally coiled *G. menardii* form 4. The unkeeled globorotaliids of the *G. scitula* group show both sinistral and dextral coiling directions. However, due to their rare occurrence, it is difficult to make a distinction in coiling preference. Neogloboquadrinids are also rare and show both coiling directions, although a sinistral coiling direction is clearly dominant. *Globigerinoides obliquus extremus* and *Sphaeroidinellopsis seminulina* are present in low numbers throughout the section, but are more common at certain levels (Fig. 4).

For this section, we estimate an age older than the LCO of *G. menardii* form 4 at ~7.51 Ma for the top of the section. The biostratigraphic evidence further points to an age younger than, at least, the FO *G. obliquus extremus* at ~8.37 Ma, and likely younger than the lro of *S. seminulina* at ~7.92 Ma.

4.2.3. Palaeo-bathymetry and depositional environment

The benthic foraminiferal assemblages of the Taounate section remain approximately the same throughout the sequence and are characterised by the following species: buliminids, e.g. *Bulimina elongata*; *Cibicides dutemplei*; *Nonion*, *Lenticulina* and *Uvigerina* spp.; *Pullenia bulloides*, *Valvulineria bradyana*. Changes in diversity and minor changes in abundances of the common species are probably related to variable preservation, changing terrigenous input, variable influx of organic matter from shallower depths and oxygenation of the sea floor. These assemblages reflect deposition in mid–outer shelf depths (100–250 m), in a relatively eutrophic environment.

4.3. Bouhaddi

4.3.1. Field observations and lithology

Bouhaddi seems to be connected to the Taounate basin on geological maps (Fig. 2), but is locally separated from the latter by the Taounate ridge (Fig. 4B, C). The Taounate ridge consists of deformed Mesozoic sediments folded in the Mesorif Nappe (Fig. 1). We collected samples and made observations at two locations: The lower part of the succession ("base" in Fig. 5A) is composed of up to 20 m thick sandstone intervals and intercalated marlstone; and the upper part ("top" in Fig. 5A) includes the uppermost marlstone and 10 to 15 m thick sandstone – lobes (Fig. 5B). Layers of the basal sandstone – conglomerate onlap against the ridge to the north (Fig. 4B), suggesting that part of this relief already existed during deposition. Paleocurrents measured in the pebbly sandstone (Fig. 5C, D) reflect a west– and southwest–directed transport (Fig. 2).

4.3.2. Biostratigraphy and age

4.3.2.1. Planktonic foraminifera. The analysed samples contain predominantly sinistrally coiled *G. menardii* form 4, some of which are similar to *G. miotumida*. Rare dextrally coiled specimens of *G. menardii* form 5 are found in the uppermost samples RTS 1–5 (Fig. 5A). The *G. scitula* group is dominantly sinistrally coiled and reveals gradual morphological changes from the low biconvex forms typical of *G. scitula* to more

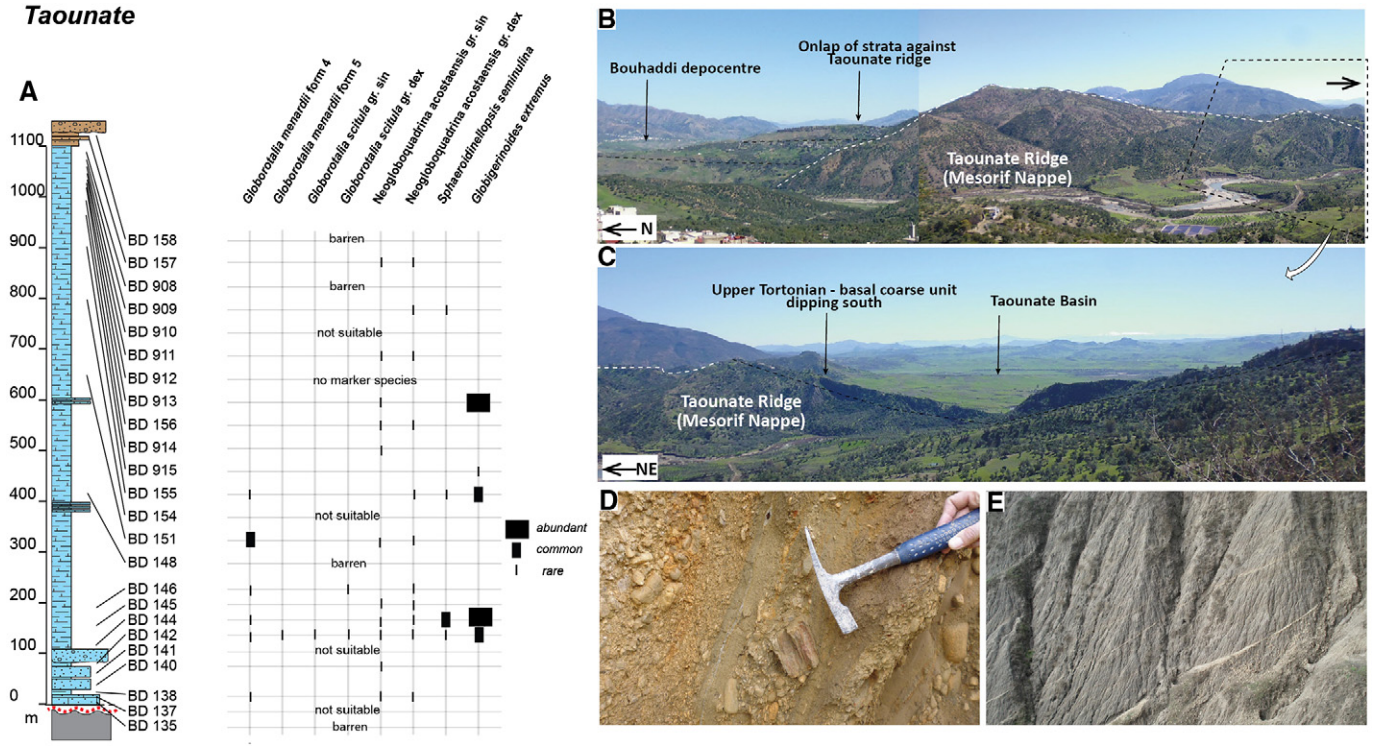

Fig. 4. Details of the Taounate section: A) Sedimentological log with distribution of planktonic foraminifera and palaeoenvironmental interpretation (legend in Fig. 6). B–C) Panoramic views taken from the town of Taounate (Fig. 2, view to the east) showing the geometric relationship between the Taounate ridge and the sedimentary infills of the Bou Haddi and Taounate depocentres. The sandstone layers of the Bou Haddi depocentre (black dotted lines) onlap on the northern side of the Taounate ridge (C), whereas the Taounate sandstone layers of the basal coarse unit are tilted indicating post-depositional uplift of the southern side of the ridge; D) Detail of the conglomerate and mudstone of the basal unit; E) Marlstone with sandstone intercalations.

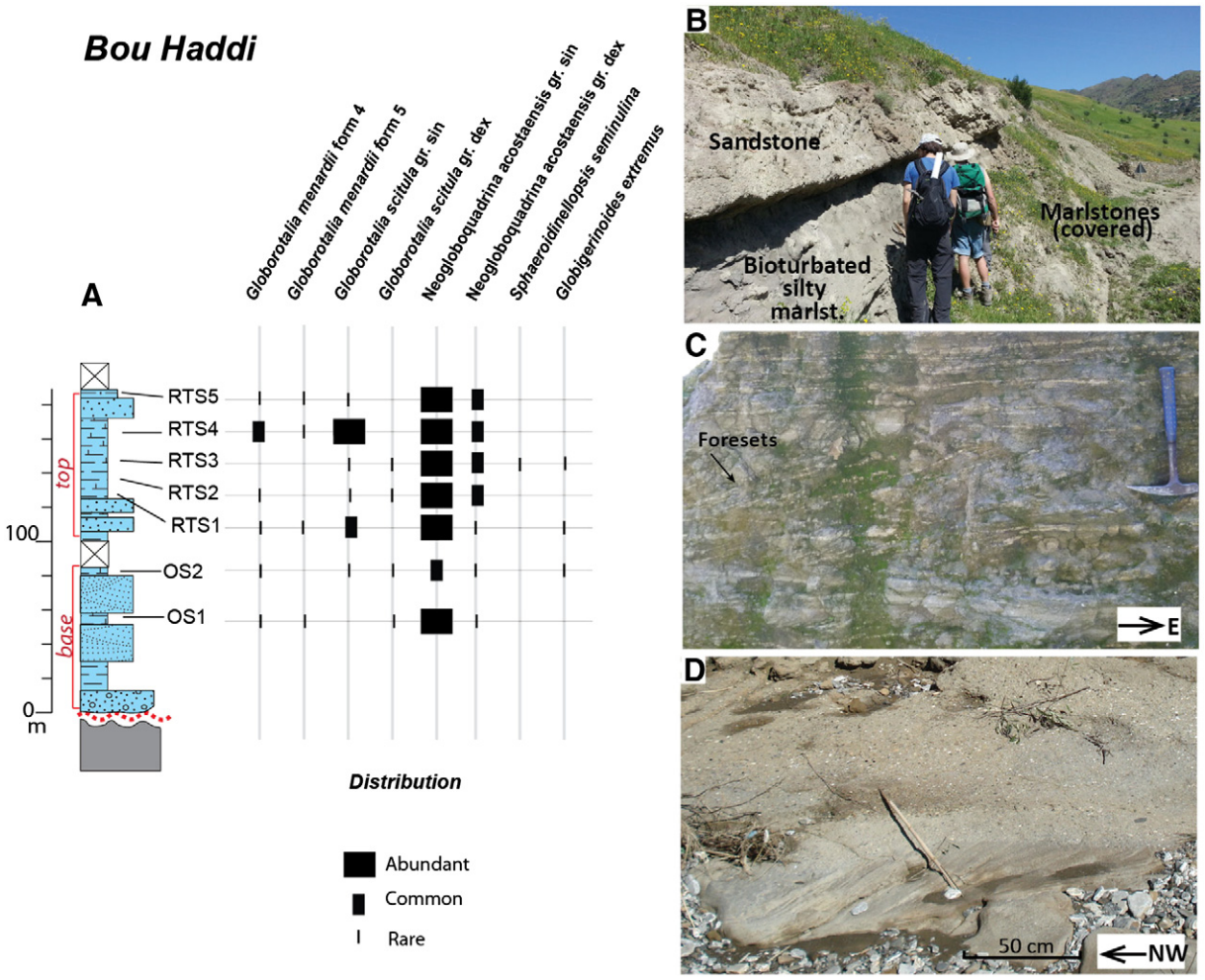

Fig. 5. Details of the Bou Haddi section: A) Sedimentological log with distribution of planktonic foraminifera and palaeoenvironmental interpretation (legend in Fig. 6); B) geometry of the sandstone intervals sandwiched in silty marlstone; C) Cross-stratification in the sandstone intervals from the base of the section; D) foresets capped by microconglomerates.

inflated biconvex forms and finally to the planoconvex inflated types typical of *Globorotalia suterae*. Predominantly sinistral neogloboquadrinids are common, while *S. seminulina* appears in low numbers in one sample only. Rare specimens of *G. obliquus extremus* are sporadically found. Relatively high number of Cretaceous-Paleogene foraminifera is present in all samples.

Based on the presence of *G. suterae* types in the *G. scitula* group, which are usually present in the latest Tortonian, and the fact that the keeled globorotaliids are dominated by typical *G. menardii* form 4 and that *G. menardii* form 5 is rare, the sediments were likely deposited in the interval between event 6 (7.58 Ma) and 4 (7.35 Ma). Note that it is not unusual to find rare specimens of *G. miotumida* (*G. dalii* type of Zachariasse, 1975) or *G. menardii* form 5 in assemblages of keeled globorotaliids that are dominated by *G. menardii* form 4 and are late Tortonian in age.

4.3.2.2. Calcareous nannofossils. In this section, calcareous nannofossils are abundant and relatively well preserved, reworking sometimes exceeding 10%. The assemblage is dominated by "very small reticulofenestrids" < 3 μm (VSR, mainly *Reticulofenestra minuta*) and minor proportions of medium-sized reticulofenestrids 3–5 μm (largely *Reticulofenestra minutula*), with some specimens of *Discoaster surculus* at the top of the section. No other marker species such as *Discoaster berggreni*, *Discoaster quinqueramus* or ceratoliths (*Amauolithus*/*Nicklithus*/*Ceratolithus*) have been identified. The dominance of VSR over medium sized reticulofenestrids was identified by Flores and Sierro (1989) just above the FO of *D. berggrenii*. Some specimens of circular *Reticulofenestra* were observed near the top of the section, but these morphotypes do no match with the characteristic forms described in the early Messinian as *Reticulofenestra rotaria* (Young et al., 1994; Raffi and Flores, 1995). For these reasons, the chronological interval we propose is late Tortonian. Per contra, the scarcity of *Discoaster* and absence of ceratoliths, could be due to an ecological restriction (these taxa are related to open-ocean environments) and for this reason do not discard a Messinian age.

4.3.3. Palaeo-bathymetry and depositional environment

All the samples are affected by re-deposition and some samples contain Cretaceous to Miocene material; however, benthic foraminifera considered to be in-situ suggest deposition at mid- shelf depth (*Cibicides ungerianus* and *C.* cf. *ungerianus*; *Cibicides lobatulus*; *Bulimina striata*; *Gavelinopsis praegeri*; *Oridorsalis umbonatus*; *Nonion fabum*; and some *Elphidium* and *Ammonia* spp.).

These assemblages suggest water depths of 100–150 m. Furthermore, fluctuating abundances of benthic foraminifera, percentage of glauconite and other sediment components together suggest repeatedly changing environments and oxygenation levels through time.

4.4. Dhar Souk

4.4.1. Lithology

The Dhar Souk section contains analogous lithofacies and lithofacies sequence than those observed in the Taounate Basin (Wernli, 1988). This section shows a prominent, tilted basal conglomerate (Fig. 6B, C) and ~1000 m thick mud-dominated succession (Fig. 6D). Vidal (1979)

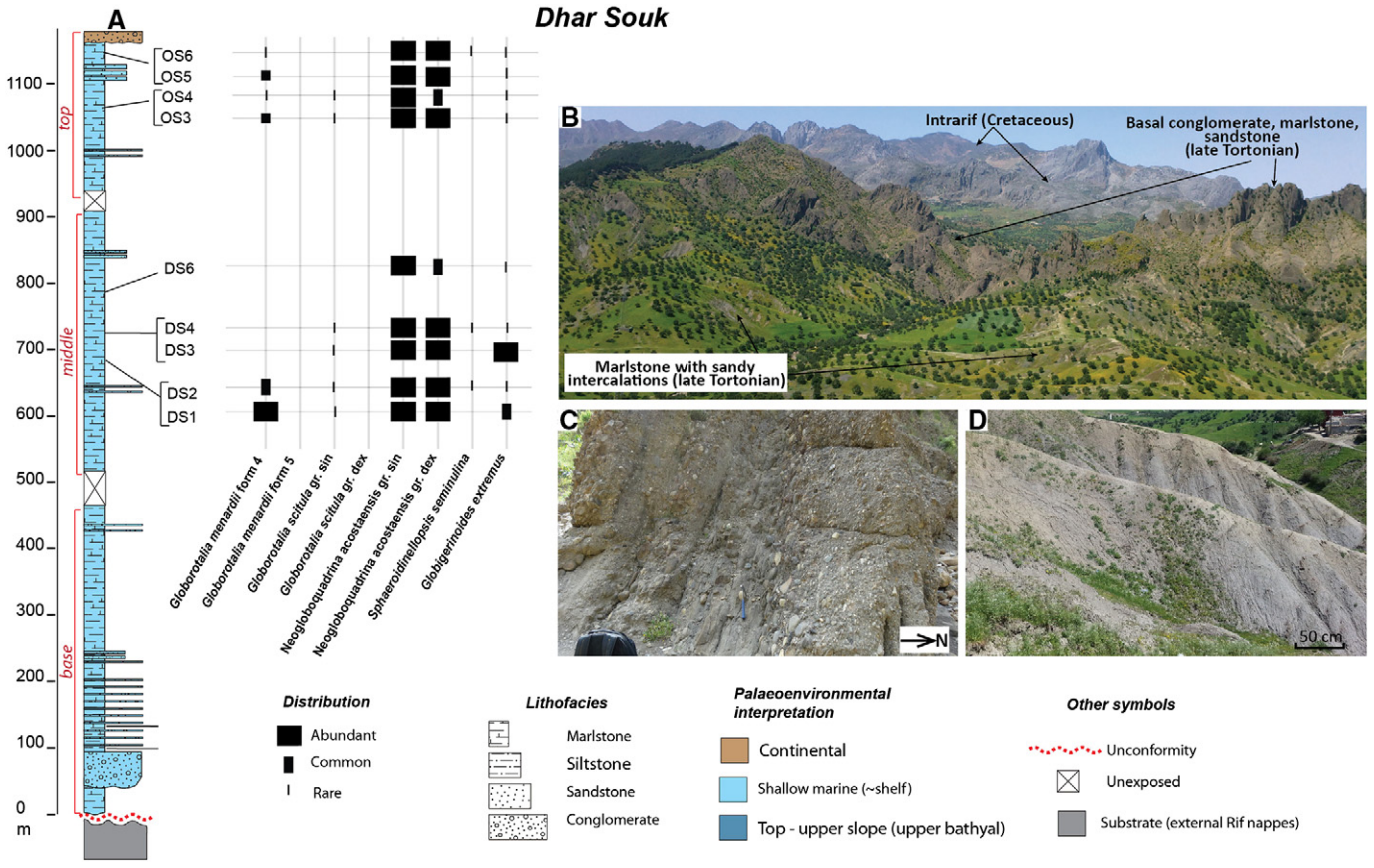

Fig. 6. Details of the Dhar Souk section: A) Sedimentological log with distribution of planktonic foraminifera and palaeoenvironmental interpretation; B) Panoramic view of the Dhar Souk section showing tilted basal conglomerates and sandstones (base) followed by mud-dominated sedimentation (middle). Picture taken from the top of the section; C) Alternations of matrix-supported conglomerates and mudstones of the basal coarse unit; D) Marlstones with irregular sandy intercalations of the middle and top parts of the section.

and Wernli (1988) report conglomerate lobes feeding the Dhar Souk depocentre from both northern and southern margins, suggesting that some topography was present on both sides of this sub–basin at times of deposition. We have not studied this basin in such high resolution to verify this information; however it could be an indication that both margins were a bathymetric high or an emergent area during the late Tortonian. Furthermore, Wernli (1988) suggests that these conglomerate lobes were indicating an overall direction of progradation towards the west–southwest (Fig. 2).

We analysed the sets of samples of Wernli (1988) and collected a number of new samples in different areas of the basin (base: DTS0–6; middle: DS1–6; top: OS3–6; Fig. 6A) to date the youngest part of the post–orogenic sedimentary succession. Sedimentation starts with high amount of gravels and pebbles (Fig. 6B, C) mixed with muddy matrix that contains foraminifera; the sequence continues with blue marlstones with irregular intercalations of sandstone beds (Fig. 6D). At the top, the sequence is truncated by Quaternary conglomerate.

Combining micropalaeontological and sedimentological information we conclude that the Dhar Souk depocentre represents a river–dominated basin, with pro-delta environments and conglomerate lobes (Fig. 6C), and where the currents (and sediment transport) where funnelled in the axial trough. The predominant direction of progradation of this basin is to the west–southwest (Wernli, 1988). This direction is in line with palaeocurrents obtained at Sidi Ali Ben Daoud.

4.4.2. Biostratigraphy and age

4.4.2.1. Planktonic foraminifera. The residues of the samples from the Dhar Souk section of Wernli (1988) were analysed, but lacked sufficient material and marker species. To date this section, we rely especially on the new samples that we collected in the middle and top parts (Fig. 6A) of the succession. Rare *G. menardii* form 4, *S. seminulina*, and sinistral *N. acostaensis* were found. These assemblages would suggest an age similar to the Taounate section, i.e. between events 8 (7.92 Ma) and 4 (7.35 Ma; Table 1).

4.4.2.2. Calcareous nannofossils. The sections studied in this sector show a low abundance of calcareous nannofossils with reworked nannoliths, sometimes over the 30%. The assemblage is dominated by VSR with occasional presence of *Discoaster* species that are in general overgrown, as well as the absence of ceratoliths. No other markers were identified. The stratigraphic framework is similar to the Bouhaddi section; the dominance of VSR over medium-sized reticulofenestrids and absence of ceratoliths indicate a late Tortonian assemblage. However, due to potential ecological restriction factors, the Messinian age cannot be excluded.

4.4.3. Palaeo-bathymetry and depositional environment

In samples collected from the middle part, the benthic foraminiferal assemblages consist of both shallow and deeper shelf taxa. Grain size sorting and differential preservation of foraminifera indicate sediment transport; consequently the shallow–water species (mainly *Ammonia* spp.) are considered to be transported downslope. Depth of deposition is estimated at mid–outer shelf (100–250 m) based on the common occurrence of cibicidids (*Cibicides ungerianus*, *C. lobatulus* and some *Cibicides dutemplei*), *Gavelinopsis praegeri*, *Nonion fabum*, *Oridorsalis umbonatus*. *Valvulineria bradyana* is common in most, and dominant in some samples. High abundances of this species are found in or near prodelta environments and mud belts associated with river plumes (e.g. Amorosi et al., 2013; Goineau et al., 2015).

In the top part (Fig. 6A), the benthic foraminiferal assemblages consist of cibicidids, (among others *C.* cf. *ungerianus*, *C. dutemplei*, *C. lobatulus*). *Gavelinopsis praegeri* and *N. fabum* are abundant and

Elphidium and *Ammonia* spp. are common. Some reworked miliolids are present. *Valvulineria bradyana* is dominant in all samples, indicating deposition in a prodelta environment. The estimated depth of deposition is 100–150 m.

4.5. Sidi Ali Ben Daoud

4.5.1. Lithology

The Sidi Ali Ben Daoud (SABD) section represents a satellite outcrop of the Dhar Souk depocentre (Fig. 2). We analysed the set samples of Wernli (1988) and collected a new set in the uppermost part (samples JJ0–7; Fig. 7A). Unconformably overlying the Mesorif Nappe of the Orogenic Wedge is an alternation of mudstone–dominated intervals containing cm–thick sandstone beds (20 to 50 m thick; Fig. 7D) and sandstone–dominated intervals with cross–stratified pebbly sandstone and conglomerates (Fig. 7B, C, E) up to 20–30 m thick. The mudstone–dominated intervals record sand deposition in cm–thick crudely graded beds (Fig. 7D). Palaeocurrent reconstructions from sole–marks in the sandstone beds show west–directed flow, whereas trough–cross bedding in the pebbly sandstone (Fig. 7C) indicates SW–directed progradation.

4.5.2. Biostratigraphy and age

4.5.2.1. Planktonic foraminifera. In the SABD section, a large number of samples are barren of microfaunal content. At levels where planktonic foraminifera are present, they are small sized and occur in low abundance. Nevertheless, the assemblages reveal marker species such as the neogloboquadrinids which show approximately equal numbers of dextral and sinistral specimens. The keeled *G. menardii* is present with specimens of form 4, while unkeeled globorotaliids (i.e. *G. scitula* group) are found in low numbers in one sample, showing both coiling directions. *Sphaeroidinellopsis seminulina* and *G. obliquus extremus* are present.

The discontinuous low frequency of *G. menardii* form 4 suggests a maximum age for the top part of the section close to event 5 (7.51 Ma), but the absence of sinistral *G. scitula* indicates an older age. On these grounds, for the SABD section we propose an age interval for deposition between lco of *S. seminulina* (7.92 Ma) and LCO of *G. menardii* form 4 (7.51 Ma).

4.5.2.2. Calcareous nannofossils. In this section, the calcareous nannofossils are scarce, sometimes in same proportion than autochthonous. No discoasters and ceratoliths have been identified. What is remarkable is the predominance of VSR over medium-sized reticulofenestrids (event placed above the FO of *D. bergrenii* – Flores and Sierro, 1989). The assemblages are overall indicative of the late Tortonian. However, as commented in Dhar Souk section, potential ecological restriction factors can be linked with the absence of marker species, and consequently the Messinian age cannot be excluded.

4.5.3. Palaeo-bathymetry and depositional environment

Benthic foraminifera are found in 6 samples and generally poorly preserved. The species found include *Ammonia beccarii*, several *Elphidium* and *Lenticulina* spp., *P. bulloides*, *Nonion commune*, *Uvigerina peregrina* and *V. bradyana*, suggesting mid-shelf depths (100 ± 50 m).

4.6. Boured

4.6.1. Lithology

Boured is a small outcrop located in a key palaeogeographic position, between the Dhar Souk Basin to the west and Arbaa Taourirt to the east (Fig. 2). The sequence is composed of marlstones and conglomerates

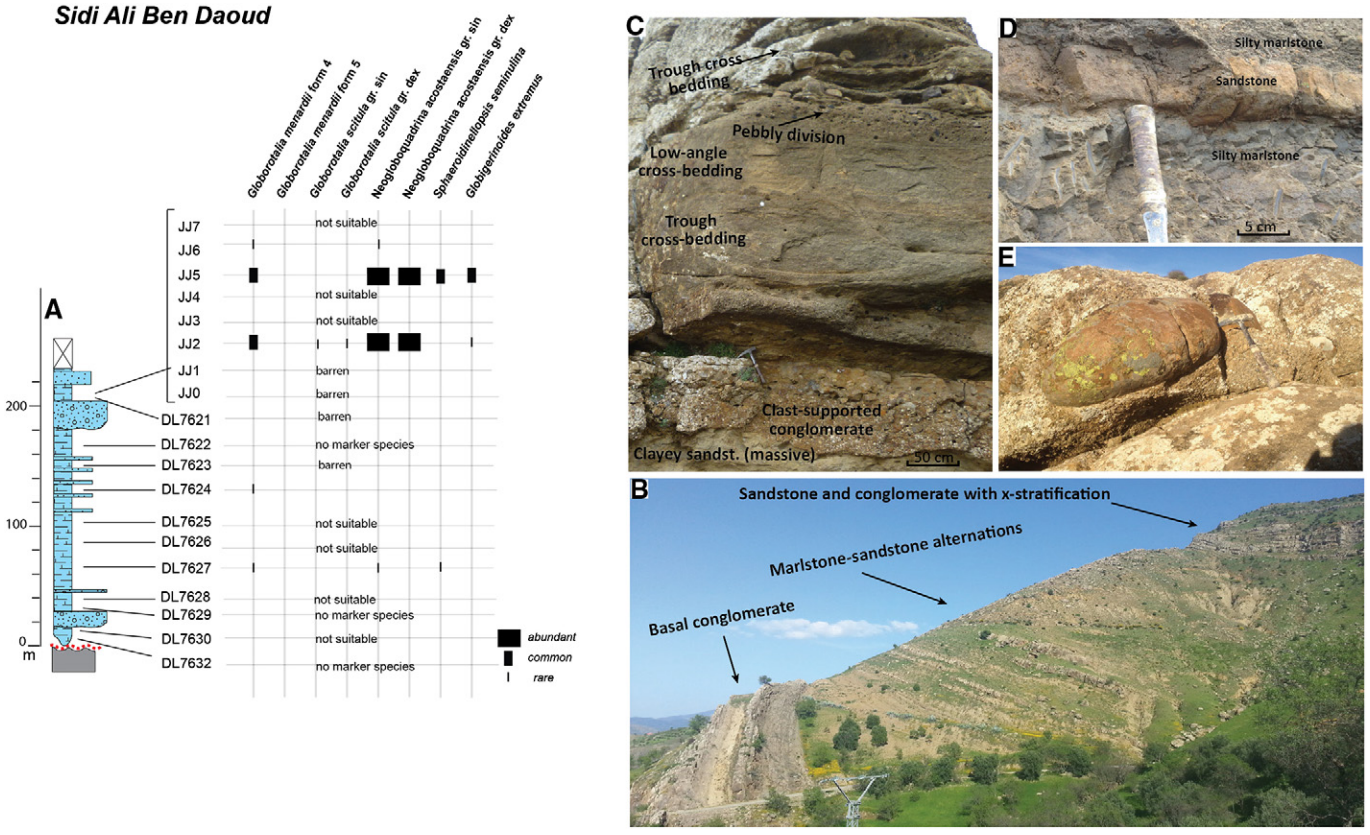

Fig. 7. Details of the Sidi Ali Ben Daoud section: A) Sedimentological log with distribution of planktonic foraminifera and palaeoenvironmental interpretation (legend in Fig. 6); B) Panoramic view of the section showing synkinematic wedge-shaped sedimentation between the basal conglomeratic unit and the following sandstone-marlstone alternations; C) Vertical relationship of sedimentary structures in the ~20 m thick sandstone-conglomerate unit at the top; D) Close-up of a turbidite intercalation in the mud-dominated interval.; E) Rounded boulder in the marine sandstone at the top of the section.

(Fig. 8A–C), locally forming channels and lobes (Fig. 8D), with a total thickness of ~150 m. Field studies and sampling for biostratigraphy were carried out by Wernli (1988) and we analysed the available samples from his collection at the Ministry of Geology in Rabat (samples DL2064–2068; 2072–2078; 2081–2086). In addition, we collected two pilot samples in the mudstones (BOU1, 2) and measured paleocurrents in marine conglomerates (Fig. 2).

4.6.2. Planktonic foraminiferal biostratigraphy and age

In the Boured basin, the planktonic foraminifera are rare, small sized and poorly preserved, often covered by detritus. An exception is sample DL 2076 (Fig. 8A), which is rich in well preserved foraminifera. The sinistrally coiled *G. menardii* form 4 specimens are found in this sample in a rare abundance, while unkeeled globorotaliids are absent through the section. Rare forms of *G. obliquus extremus* and sinistrally coiled neogloboquadrinids are found, whereas *S. seminulina* is common.

The assemblages suggest the section was deposited between the lro of *S. seminulina* at 7.92 and the LCO of *G. menardii* form 4 at 7.51 Ma.

4.6.3. Palaeo-bathymetry and depositional environment

Benthic foraminifera are present in two samples and suggest mid–shelf depths (100 ± 50 m), based on the occurrence of *Elphidium*, *Lenticulina* and *Uvigerina* species, *Ammonia beccarii*, *V. bradyana*, *N. commune* and *Pullenia bulloides*.

4.7. Aarba Taourirt composite

4.7.1. Field observations and lithology

The Arbaa Taourirt composite section (Fig. 9A) is located approximately 25 km away from the modern Mediterranean Coast. Previous studies (Frizon de Lamotte, 1981; Wernli, 1988; Achalhi et al., 2016) report that unconformably overlying the orogenic wedge and the Nekor Fault zone are the following three clastic units, from base to top: 5 to 10 m thick conglomerates (Fig. 9D), ~70 m thick marlstones (Fig. 9B, C), ~100 m thick marine conglomerates and sandstones (Fig. 9B). The top unit reflects dominant N– and NW–directed sediment transport possibly associated with the inflow of oceanic currents in the NRC (Achalhi et al., 2016).

The North Arbaa and Azroû Zazîrhîne (Fig. 9A) were previously presented in Achalhi et al., 2016, whereas Tarhzout Ntassa is analysed for the first time. We only targeted the mudstone intervals; information and palaeoflow indicators (Fig. 2) from the uppermost ~100 m thick conglomerate and sandstone is based on the data of Achalhi et al. (2016). In addition, the mud–dominated interval contains a variable amount of silt, and shows 5 to 50 cm thick intercalations of sandstone containing ripple cross–laminations and mud–drapes; a typical sequence of these beds shows the succession of, from base to top: silty mud, ripple cross–laminated sand, parallel–laminated sand and silty mud (Fig. 9E).

Tarhzout Ntassa section consists of ~30 m thick mudstone with two sandstone intercalations cropping out to the east of the Nekor River, ~2 km northeast of North Arbaa section, separated from the latter by Quaternary river erosion.

4.7.2. Biostratigraphy and age

4.7.2.1. Planktonic foraminifera. The planktonic foraminiferal assemblage in the lowermost part of the section contains a large number of keeled globorotaliids. A higher variability in taxa distinguished a mixture of more typical *G. menardii* form 4, and specimens resembling *G. miotumida*. The unkeeled *G. scitula* group is rare and sinistrally coiled, except for one sample (TN 10) in which it is relatively common. The neogloboquadrinids group is common and shows a clear sinistral coiling preference, although dextrally coiled specimens are present. Specimens of typical *G. obliquus extremus* and *S. seminulina* are rare. Forms of reworked Cretaceous foraminifera are found throughout the section. By contrast, the *G. menardii* group is almost completely missing in the upper part of the marly succession, and only a single specimen of *G.*

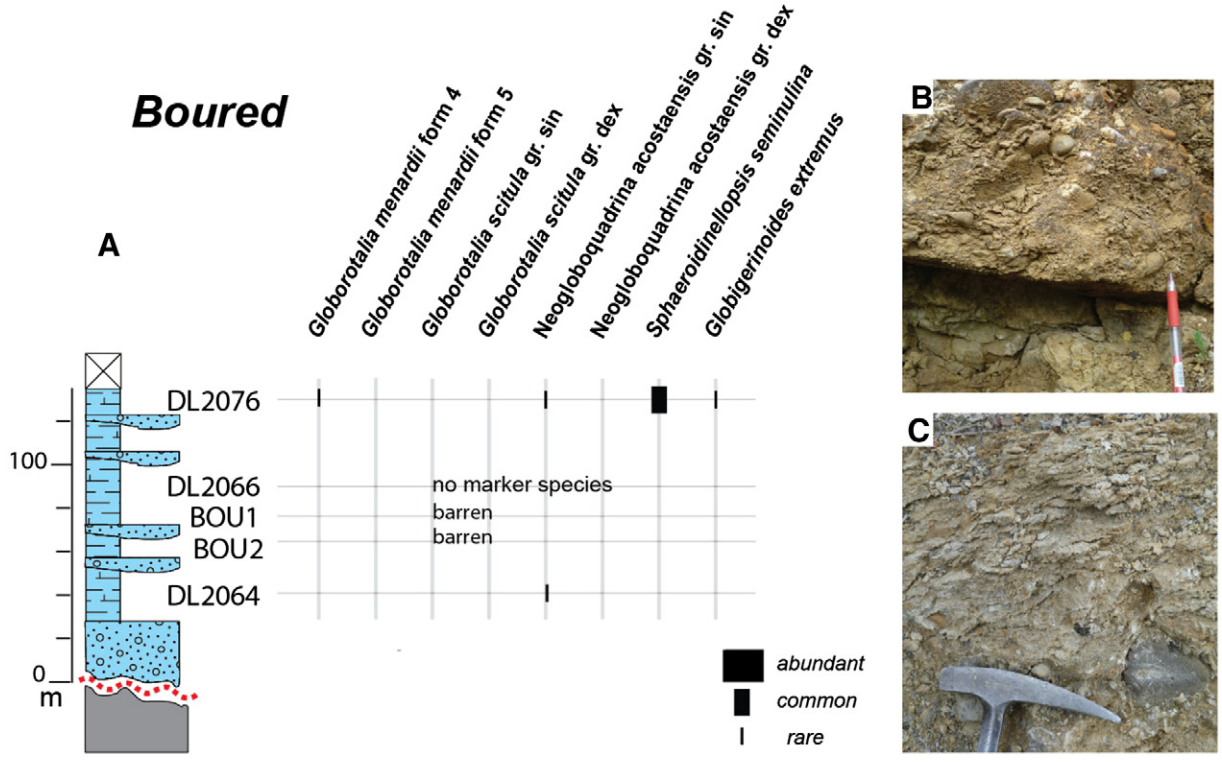

Fig. 8. Details of the Boured section: A) Sedimentological log with distribution of planktonic foraminifera and palaeoenvironmental interpretation (legend in Fig. 6); B) marine marls truncated by marine conglomerates; C) marine marls including pebbles from the nearby paleomargins.

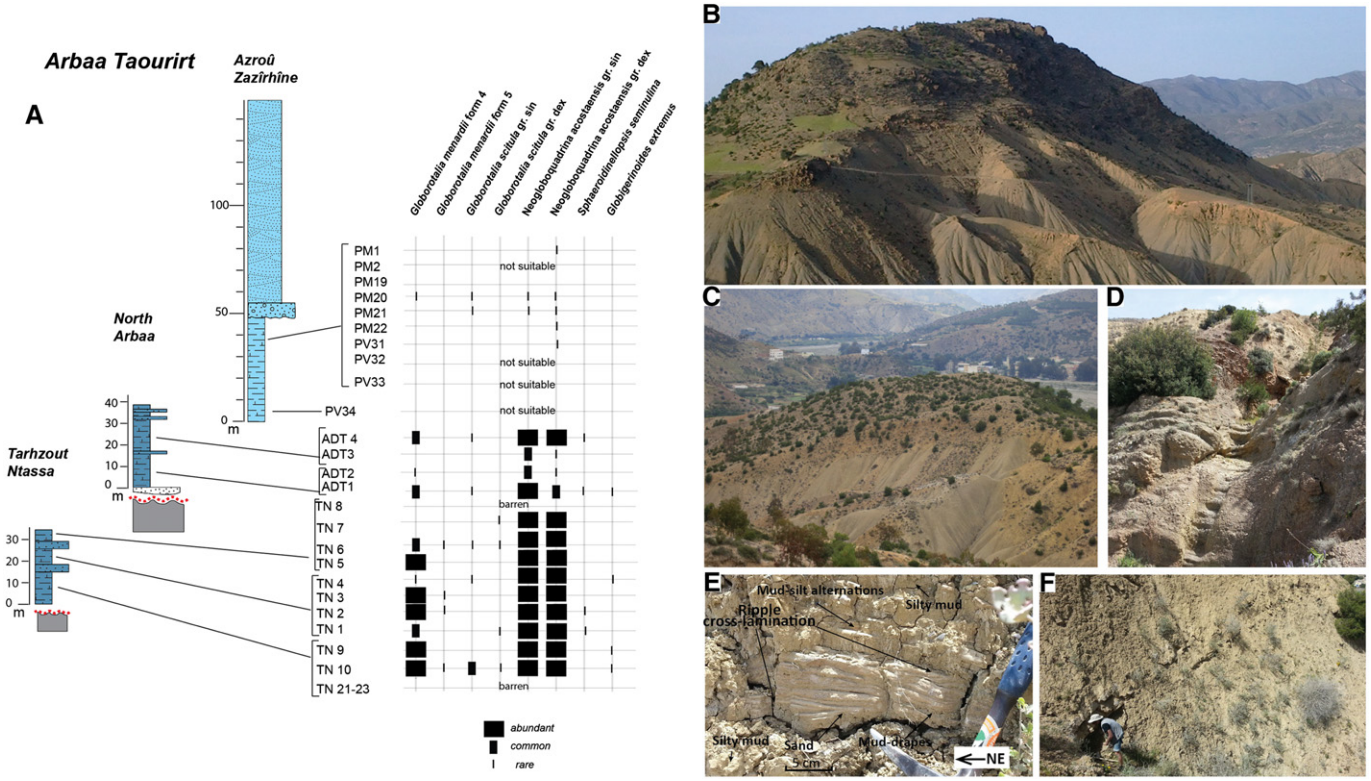

Fig. 9. Details of the Arbaa Taourirt composite section: A) Sedimentological log with distribution of planktonic foraminifera and palaeoenvironmental interpretation (legend in Fig. 6); B) outcrop view of the Azroû Zazîrhîne section; C) outcrop view of the Tarhzout Ntassa section (in the background, the village of Arbaa Taourirt); D) Basal conglomerate at the North Arbaa section; E) Possible contourite feature at the North Arbaa section; F) sandstone interval in the marine marls of the North Arbaa section.

menardii form 4 is found. Specimens of the *G. scitula* group are rare and sinistrally coiled. Neogloboquadrinids are represented by dextrally coiled specimens and *S. seminulina* is present.

The assemblages suggest an age between 7.80 and 7.35 Ma. Event 5 (7.51 Ma) is probably located towards the base of the section whereas the middle and upper part of the succession were probably deposited between 7.51 and 7.35 Ma, because *G. menardii* form 4 is either rare or absent.

In Tarhzout Ntassa, the planktonic foraminiferal assemblages contain the marker species of the predominantly sinistrally coiled neogloboquadrinids, common *G. menardii 4*, rare to common *G. scitula*, including typical *G. suterae*. *G. obliquus extremus*, *S. seminulina* are present. The maximum age of this section is constrained by event 7 (7.80 Ma). Minimum age is, like North Arbaa, constrained by event 5 (7.51 Ma).

4.7.2.2. Calcareous nannofossils. An abundant record of calcareous nannofossils shows assemblages dominated by VSR over medium sized reticulofenestrids, with the occasional presence of *D. quinqueramus* and *D. berggrenii*. Flores and Sierro (1989) identified a reversal in the domain of the VSR vs. medium-sized reticulofenestrids just after the FO of *D. berggrenii* calibrated at 8.29 Ma (Lourens et al., 2004).

Discoaster surculus is first recorded in sample TN2. Other *Discoaster* species are rare and no ceratoliths have been found. The first common occurrence (FCO) of *D. surculus* is placed at 7.79 Ma and the FO of *Amaurolithus* spp. at 7.42 (Lourens et al., 2004; Raffi et al., 2006), in the latest Tortonian. However, the Messinian stage can still be consider as a possibility. It should be noted that an ecological absence of *Amaurolithus*, particularly *Amaurolithus delicatus* (FO at 7.22 Ma; Lourens et al., 2004), cannot be ruled out since this species is usually rare, linked to open ocean environment.

On the other hand, the studied interval coincides with the *Reticulofenestra pseudoumbilicus* paracme (sensu Raffi et al., 2006), characterised by the absence of forms of this species larger than 7 μm. However, reworking in this interval exceeding sometimes 20% precludes an accurate definition of this biostratigraphic interval.

4.7.3. Palaeo-bathymetry and depositional environment

Benthic foraminiferal assemblages differ slightly between (i) Tarhzout Ntassa/North Arbaa and (ii) Azroû Zazîrhîne, indicating a slight shallowing–upward trend. Tarhzout Ntassa and North Arbaa assemblages contain inner shelf species (*Ammonia*, *Elphidium* and/or *Rosalina*, discorbids) as well as species occurring on the deeper shelf and upper slope (*C. dutemplei*, *C. pachyderma*, *C. ungerianus*, some *Cibicidoides kullenbergi*, *Planulina ariminensis*, *Uvigerina peregrina*, and some *V. bradyana*). Considering that some transport of material is evident in most samples (based on grain size sorting and differential preservation of foraminifera), the shallow–water species are considered to be transported. Estimated water depth is between 150 and 300 m (outer shelf/upper slope).

Azroû Zazîrhîne assemblages contain fewer shallow–water species but apart from abundant *U. peregrina*, the deeper–water species (e.g. *C. kullenbergi*; *P. ariminensis*) are absent. The depth of deposition is therefore estimated at mid–outer shelf depths (~100–200 m).

4.8. Msila

4.8.1. Field observations and lithology

The Msila section consists of an alternation of marlstone and sandstones that unconformably overlie the Mesorif Nappe of the orogenic wedge. This section, assigned to Upper Miocene post–nappe cover in the regional geological map (Suter, 1980), was targeted to better constrain its age as it may represent a key point for palaeogeography, being located along the Mesorif–Prerif boundary that could have tectonically–controlled a marine connection between the eastern edge of the Taounate Basin and the Taza area.

4.8.2. Planktonic foraminiferal biostratigraphy and age

The lower part of the succession (samples MS 1–4) contains assemblages characterised by mixed Miocene and Eocene planktonic foraminifera. The specimens are badly preserved. *G. apertura* and *G. sacculifer* groups were identified. Neither keeled nor unkeeled globorotaliids were present, except for *Globorotalia peripheroronda* which is Serravallian in age. The Neogloboquadrinids are represented by *P. mayeri–siakaensis* types that indicate ages older than Tortonian. The absence of typical Tortonian species and the presence of *Globigerinoides altiperturus* suggest that the sediments are of Early to Middle Miocene age.

5. Seismic stratigraphy of the Taounate basin

Part of the Taounate sedimentary succession is now better dated and allows to correlate outcrop to seismic data. Samples taken in the Taounate section correspond to the two uppermost units observed in the subsurface (see below). Two representative seismic lines cross the Taounate Basin and illustrate its structure at depth. Given the new dating of the surface sediments carried out in this paper we are able to provide a new interpretation of the tectono–sedimentary evolution of the area, modified after larger-scale analyses of field kinematics and seismic profiles in the Rif foreland (Capella et al., 2017a, 2017b, 2017c). At the base of the Taounate sedimentary infill, unit U1 consists of packages of high–amplitude reflectors that are slightly divergent. This discordance reflects a clear synkinematic character of the unit U1, also expressed by lateral variations of thicknesses (Fig. 10). We suggest that this synkinematic character resulted from coeval movements along the basin flanks due to thin–skinned fault–propagation in the underlying Mesorif unit. The sub–units U1A thickens towards the WNW in line TAO–1 and SSW in line TAO–2.

Taounate could then be interpreted as a piggy–back basin during the time of deposition of U1. In profile TAO–2, it is possible to detect a change in lateral thickening of this unit U1 in correspondence with sub–units B and C. This change is only detected by line TAO–2 due to its transverse orientation. This change adds weight to the hypothesis of the southward fault–propagation, as unit B and C infill the space created by earlier contraction and were possibly controlled by a new thrust front to the south.

U2 is composed of parallel and high–amplitude reflectors and attest to a post–kinematic phase. Line TAO–1 indicates that the linear extent of U2 is approximately 30 km, in contrast with the 15 km of U1. U2 is tilted at the flank margins in TAO–2 as a result of post–depositional contraction. U3 is separated from the underlying U2 by an unconformity and shows moderate synkinematic character expressed by lateral variations in thickness. This character is particularly clear in line TAO–1, whereas the location of U3 in line TAO–2 is only speculative and result of correlation with intersecting longitudinal lines. U3 would seem to thicken towards the WNW, therefore suggesting a controlling fault located to the east of the basin.

To sum up, the following can be inferred on the basis of the stratal geometry: (i) during the deposition of U1 accommodation space in the NRC was controlled by south–westward fault propagation. Over the time an increase in accommodation space is recorded by the km wider extent of the overlying units. Steep and faulted basin margins generate coarse deltaic systems, which feed deeper basinal system composed of alternations between marlstones and coarser clastics. In these prodelta and outer shelf environments (see Sections 4.2 and 4.3) both seaway parallel and transverse turbidity currents can occur; (ii) during the deposition of U2 the NRC was at its maximum extent; (iii) renewed contraction possibly occurred during the deposition of U3, restricting the basin and leading to its closure.

6. Discussion

6.1. Closure of the NRC

Application of the astrobiochronologic framework based on the assemblage-based species concept of planktonic foraminifera marker species indicates that the marine successions in the studied Intramontane

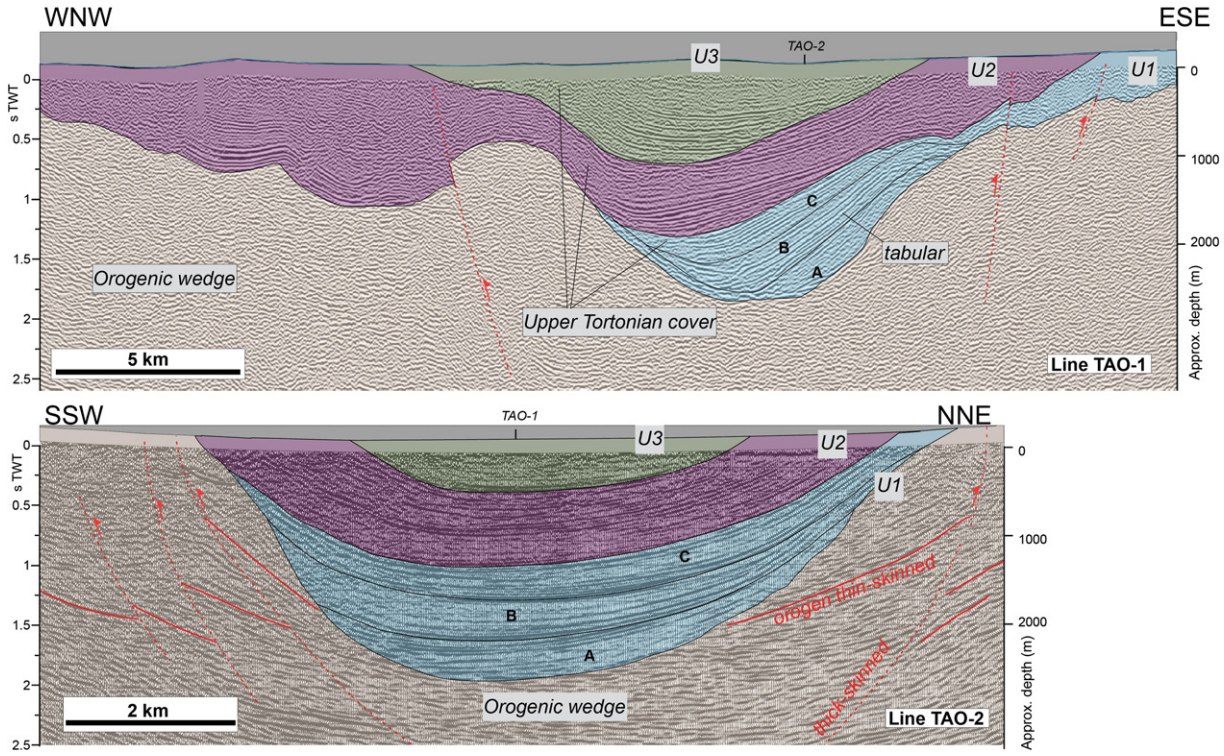

Fig. 10. ONHYM multichannel seismic profiles crossing the Taounate Basin. Depth in m is derived from seismic velocities presented in Zizi (1996). Average velocities are 2730 m/s for the Upper Miocene Blue Marl Formation, leading to 1365 m/s twtt. Locations of lines in Fig. 2.

Basins, with the possible exception of Arbaa Taourirt, are invariably late Tortonian in age and that, in contrast with previous age models (Feinberg, 1986; Wernli, 1988; Samaka et al., 1997), the Messinian is not reached. Such a late Tortonian age is based on the morphology of the keeled globorotaliids, which following the assemblage approach belong to *G. menardii* form 4, in combination with the dominantly sinistrally coiled specimens of the *G. scitula* group, which include types that belong to *G. suterae*.

However, it is also likely that at least some of the marine successions will have continued into the Messinian, as these are capped by erosive contacts and a transition to very shallow marine and continental deposits is only recorded at Taounate (Fig. 4A). Nevertheless, the benthic foraminifera indicate a shallowing of about 50–100 m in the upper part of the marine sections in two cases, from 150–300 m to 100–200 m in Arbaa Taourirt, and from 100–250 m to 100–150 m in Dhar Souk.

Furthermore sedimentation rates are very high with approximately 1 million years (~8.5 to ~7.5 Ma) represented by ~1000 m of open marine sediments, leading to a sedimentation rate of at least 100 cm/kyr. This combination of late Tortonian basin restriction detected from seismic profiles (Fig. 10), shallowing trends inferred from sedimentology (Achalhi et al., 2016), and high sedimentation rates makes it rather unlikely that the (open) marine sedimentation will have continued into middle to late Messinian. Assuming that a maximum of 500 m of the marine succession has been eroded, and that the FCO of *G. menardii* form 5 is not reached, we can roughly estimate that the top of the marine successions would not have had an age younger than ~7.0 Ma. One may argue that the inferred sedimentation rate may have been reduced during the transition from deep marine to shallow marine sedimentation, but even in that case it is unlikely that the marine connection through the NRC would have remained in existence during the MSC.

In the Arbaa Taourirt Basin, ~100 m thick shallow marine calcarenites with an estimated paleowater-depth of 90 m overlie marine marls (Achalhi et al., 2016). Keeled globorotaliids in samples from the marls in this section are dominantly sinistrally coiled, but reveal a mixture of *G. menardii* form 4 and *G. miotumida* types that we interpreted as to indicate a late Tortonian age. This assessment is in agreement with the calcareous nannofossils assemblage observed dominated by VSR over the medium-sized reticulofenestrids and absence of *Amaurolithus* spp.

However, a late Tortonian age is at odds with the calcareous nannofossils biostratigraphy of Achalhi et al. (2016), which indicates a partly Messinian age for the same sediments. According to these authors, their finding of *Amaurolithus primus* marks an age younger than 7.42 Ma (i.e. the age of the FO of *A. primius* in the Mediterranean – Lourens et al., 2004, Raffi et al., 2006). Nonetheless, if the additional presence of *Amaurolithus delicatus* is taken into account, as indicated in their Fig. 14, most of the sediments would have to be younger than 7.22 Ma and, hence, of early Messinian age. In that case, it is likely that the sinistrally coiled keeled globorotaliids found in our study belong to the *G. miotumida* group rather than to *G. menardii 4*. Nevertheless, it is remarkable that Amaurolithus has not been found in our samples from Arbaa Taourirt. In principle, the absence of ceratoliths may be explained by ecological exclusion, and their abundance is usually low. Moreover, as mentioned before, this is not in agreement with the calcareous nannofossil data presented in Achalhi et al. (2016). This discrepancy may be explained by the different counting techniques used in the two studies. For this reason, we carried out an additional check on ceratoliths especially in our samples of Arbaa Taourirt, Oued Sra (Dhar Souk) and Bou Haddi, but again not a single specimen of Amaurolithus was found. This observation is consistent with our assessment of a late Tortonian age for the same sediments. Note that an early Messinian age is difficult to reconcile with their correlation of unconformity-bound units between Arbaa Taourirt and the Boudinar basin near the Mediterranean coast (see Achalhi et al., 2016). According to these correlations, the marls of Arbaa Taourirt belong to their Sub-Unit 2a, which is supposed to be older than 7.15 Ma and does not contain *A. delicatus* in the supposedly equivalent parts of the sections in the Boudinar basin.

We conclude that the marine sedimentation in the NRC continued into the youngest part of the Messinian, but ended around 7.0 Ma. The Arbaa Taourirt basin may have acted as an embayment of the Mediterranean rather than being part of a continuous marine connection to the Atlantic, in case the biostratigraphic results of Achalhi et al. (2016) prove to be correct.

In our view, the NRC was not composed of individual interconnected basins but likely developed as a single, wedge-top basin where orogen-parallel flow was controlled by the oblique axis of the basin and limited by thrust-barriers. There is no evidence that each intramontane basin acted as an individual basin during deposition, as lateral facies variations are essentially lacking (e.g., coastal marine facies near the palaeo-margins); however, such tectonically-controlled basins can show talus-cones and submarine deltas that extend from coastal areas down to several hundred metres depth (e.g., Reading and Collinson, 1996; Mutti et al., 2003).

Dhar Souk is a syncline where sandstone, conglomerate and marl beds are deformed and truncated by an unconformity. The Taounate basin reveals upper Tortonian deep-marine marls or sandstones, but no coastal facies at its margins. Boured section comprises conglomerate and marl that have been intensively eroded. The system of interconnected depocentres was later flooded by rapid subsidence (corresponding to U2 in Fig. 10), and disconnected in the late Tortonian phase of uplift (U3 in Fig. 10).

In previous studies, the uplift of the Taounate basin along high-angle faults was linked either to inversion of extensional structures (Samaka et al., 1997) or to the onset of thick-skinned tectonics as in other part of the Rif foreland (Capella et al., 2017b). The two seismic profiles presented in this paper allow dating more accurately the restriction of the Taounate Basin by identifying a spatially limited depositional unit that likely followed an event of uplift (U3). Note that this interpretation differs from that of Capella et al. (2017b) in which only two units were recognised. Assuming that U3 corresponds to the onset of phase-3 (thick-skinned tectonics) proposed in Capella et al. (2017b), a connection through these basins could have persisted only for a short time after the enhanced rates of uplift occurred. Comparison with the marine successions exposed in the South Rifian Corridor, such as Taza-Guercif, reveal a rather similar picture with a marked shallowing in latest Tortonian and a closure of the marine connection in the earliest Messinian (Krijgsman et al., 1999; Capella et al., 2017a, in revision). In addition, no indications have been found for renewed subsidence and a marine transgression/invasion following the earliest Messinian.

These results strengthen the hypothesis proposed by Achalhi et al., 2016 that the NRC did not play a role in the MSC, by proposing that closure occurred at ~7 Ma, which is one Myr older than the onset of gypsum deposition (Roveri et al., 2014). The closure of the South Rifian Corridor was recently dated at 7 ± 0.1 Ma (Capella et al., 2017a, in revision) (Fig. 11).

Therefore, another seaway must have been open until at least 5.5 Ma to supply the inflow of seawater required for gypsum and halite saturation (e.g., Krijgsman and Meijer, 2008). The only Betic seaway that could have played a role in the Messinian was the Guadalhorce Strait in the western Betics (Martín et al., 2001); however, recent biostratigraphic dating showed that the sedimentary remnants of the Western Betic marine passages are late Tortonian in age (Van den Berg, 2016; Van der Schee, 2016, PhD thesis) consistently with the biochronology proposed with the NRC in this study. The sole option for a middle-late Messinian connection in the Western Mediterranean area remains the Strait of Gibraltar, an option that has been already put forward by several studies (Krijgsman et al., 1999; Flecker et al., 2015; Achalhi et al., 2016; Capella et al., 2017a, in revision) but not really explored and quantified yet (Fig. 12).

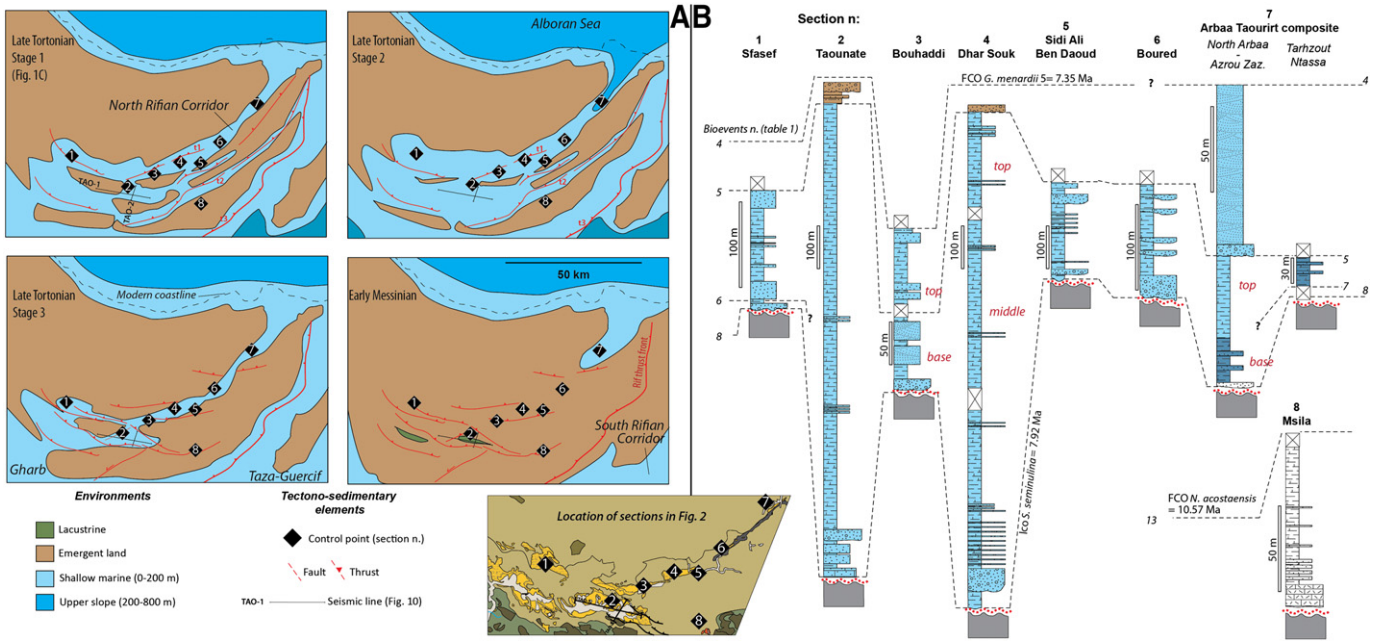

Fig. 11. (A) Summary of the palaeogeographic evolution of the North Rifian Corridor during the late Tortonian. (B) Overview of the stratigraphic logs of the studied sections and proposed correlation based on the bioevents shown in Table 1.

7. Conclusions

The open and relatively deep marine sediments deposited in the core of the NRC are all late Tortonian in age, predating the *G. menardii* form 5 FCO at 7.35 Ma. The assemblages of the planktonic foraminifera and calcareous nannoplankton thus reveal that contrary to previous age models the Messinian is not reached in the NRC. This dating would not have been possible without the application of a high-resolution astrobiochronology using planktonic foraminifera and an assemblage-based taxonomic concept.

The top parts of the marine successions have invariably been removed by erosion, suggesting that the marine sedimentation may

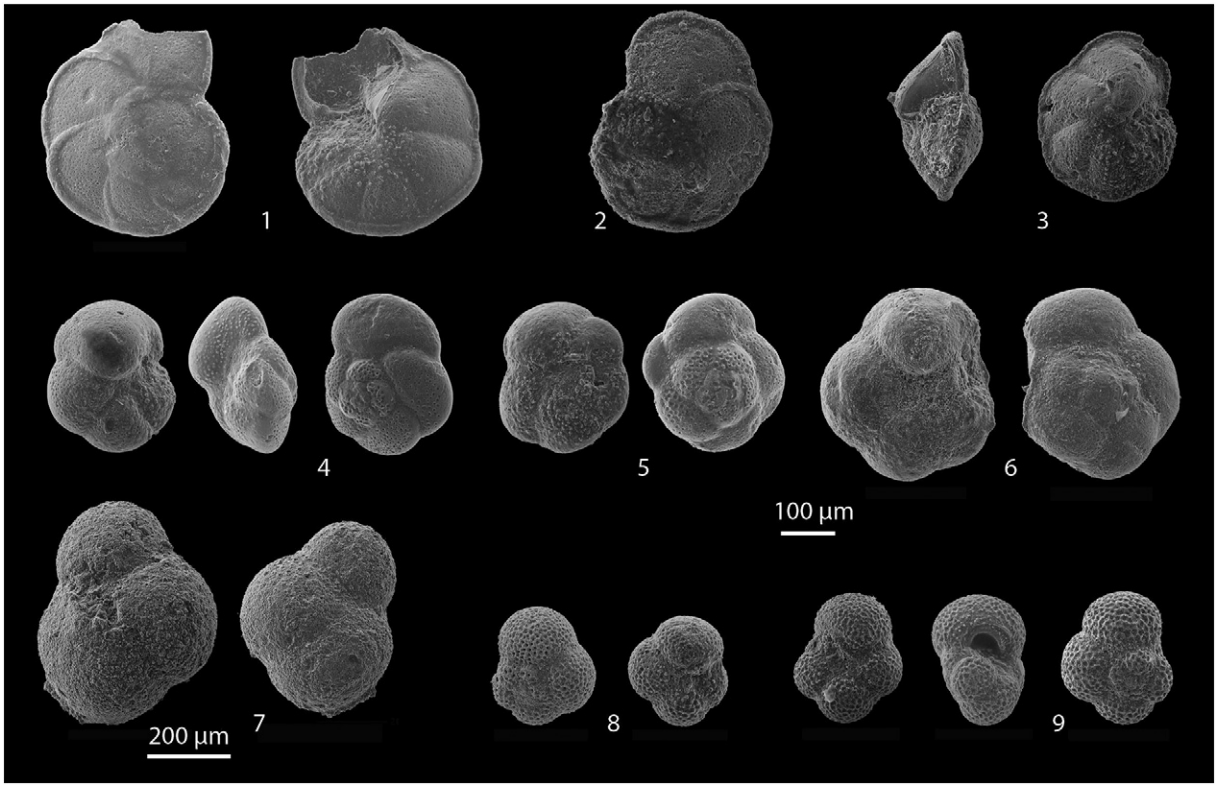

Fig. 12. Scanning electron micrographs of planktic marker species of the late Miocene. 1: *Globorotalia menardii* form 5 (Bouhaddi section); 2, 3: *Globorotalia menardii* form 4 (Aarba Taourirt section); 4–6: Specimens of *Globorotalia scitula* group, most of them were identified as *G. suterae*; 7: *Sphaeroidinellopsis seminulina*; 8, 9: Variation in *Neogloboquadrina acostaensis* group. Scale bar 100 µm, exception 7: scale-bar 200 µm.

have continued into the Messinian. However, the observed high sedimentation rates in combination with the shallowing upward trend in some of the successions below the overlying erosional surface indicates that this marine sedimentation likely ended already in the early Messinian around 7.0 Ma.

Our integrated dataset suggests that the NRC was rapidly uplifted after the deposition of the youngest rocks of late Tortonian and possibly earliest Messinian age. A connection through these basins could have persisted only for a short time after the enhanced rates of uplift started. The NRC thus did not form the long-lasting connection with the open ocean that is needed to supply the necessary salts for the deposition of the thick evaporite successions of the MSC in the Mediterranean. Therefore, Messinian connections through the Gibraltar Straits are proposed as the most likely solution to the missing gateway problem of the MSC.

Acknowledgments

This research has received funding from the People Programme (Marie Curie Actions) of the European Union's Seventh Framework Programme FP7/2007–2013/ under REA Grant Agreement No. 290201 (MEDGATE). We thank ONHYM for providing field assistance and unpublished datasets; B. van den Berg, E. Dmitrieva for joining the fieldwork; R. Wernli for sending his manuscript and the kind reply; E. C. Rjimati and F. Bouyahyaoui (Geological Institute of Morocco) for granting access to samples collections and for their availability and support during our stay. Journal reviews by Ed. Thierry Correge, André Michard and an anonymous reviewer are gratefully appreciated, and their comments helped us to improve the manuscript.

References

Achalhi, M., Münch, P., Cornée, J.J., Azdimousa, A., Melinte-Dobrinescu, M., Quillévéré, F., Drinia, H., Fauquette, S., Jiménez-Moreno, G., Merzeraud, G., Moussa, A.B., El Karim, Y., Feddi, N., 2016. The late Miocene Mediterranean-Atlantic connections through the North Rifian Corridor: new insights from the Boudinar and Arbaa Taourirt basins (northeastern Rif, Morocco). Palaeogeogr. Palaeoclimatol. Palaeoecol. 459, 131–152.

Aït Brahim, L., Chotin, P., 1989. Genèse et déformation des bassins néogènes du Rif central (Maroc) au cours du rapprochement Europe-Afrique. Geodin. Acta 3, 295–304.

Amorosi, A., Rossi, V., Vella, C., 2013. Stepwise post-glacial transgression in the Rhône Delta area as revealed by high-resolution core data. Palaeogeogr. Palaeoclimatol. Palaeoecol. 374, 314–326.

Asebriy, L., Bourgois, J., Cherkaoui, T.E., Azdimousa, A., 1993. Evolution tectonique récente de la zone de faille du Nékor: importance paléogéographique et structurale dans le Rif externe, Maroc. J. Afr. Earth Sci. 17, 65–74.

Capella, W., Barhoun, N., Flecker, R., Hilgen, F.J., Kouwenhoven, T., Matenco, L.C., Sierro, F.J., Tulbure, M.A., Yousfi, M.Z., Krijgsman, W., 2017a. Palaeogeographic evolution of the late Miocene Rifan Corridor (Morocco): reconstructions from surface and subsurface data. Earth-Sci. Rev. (in revision).

Capella, W., Hernández-Molina, F.J., Flecker, R., Hilgen, F.J., Hssain, M., Kouwenhoven, T.J., van Oorschot, M., Sierro, F.J., Stow, D.A.V., Trabucho-Alexandre, J., Tulbure, M.A., de Weger, W., Yousfi, M.Z., Krijgsman, W., 2017b. Sandy contourite drift in the late Miocene Rifian Corridor (Morocco): reconstruction of depositional environments in a foreland-basin seaway. Sediment. Geol. 355, 31–57.

Capella, W., Matenco, L., Dmitrieva, E., Roest, W.M., Hessels, S., Hssain, M., Chakor-Alami, A., Sierro, F.J., Krijgsman, W., 2017c. Thick-skinned tectonics closing the Rifian corridor. Tectonophysics 710–711, 249–265.

Chalouan, A., Michard, A., Kadiri, K.E., Negro, F., Frizon de Lamotte, D., Soto, J.I., Saddiqi, O., 2008. The Rif Belt. In: Michard, A., Saddiqi, O., Chalouan, A., Frizon de Lamotte, D. (Eds.), Continental Evolution: The Geology of Morocco. Springer, Berlin Heidelberg, pp. 203–302.

Cornée, J.J., Roger, S., Münch, P., Saint Martin, J.P., Feraud, G., Conesa, G., Pestrea-St Martin, S., 2002. Messinian events: new constraints from sedimentological investigations and new Ar-40/Ar-39 ages in the Melilla-Nador Basin (Morocco). Sediment. Geol. 151, 127–147.

Cornée, J.J., Münch, P., Achalhi, M., Merzeraud, G., Azdimousa, A., Quillévéré, F., Melinte-Dobrinescu, M., Chaix, C., Moussa, A.B., Lofi, J., Séranne, M., 2016. The Messinian erosional surface and early Pliocene reflooding in the Alboran Sea: new insights from the Boudinar basin, Morocco. Sediment. Geol. 333, 115–129.

Crespo-Blanc, A., Frizon de Lamotte, D., 2006. Structural evolution of the external zones derived from the Flysch trough and the South Iberian and Maghrebian paleomargins around the Gibraltar arc: a comparative study. Bull. Soc. Geol. Fr. 177, 267–282.

Cunningham, K.J., Benson, R.H., Rakic El Bied, K., McKenna, L.W., 1997. Eustatic implications of late Miocene depositional sequences in the Melilla Basin, northeastern Morocco. Sediment. Geol. 107, 147–165.

Dennison, J.M., Hay, W.W., 1967. Estimating the needed sampling area for subaquatic ecological studies. J. Paleontol. 4 (3), 706–708.

Feinberg, H., 1986. Les séries tertiaires des zones externes du Rif (Maroc); biostratigraphie, paléogéographie et aperçu tectonique. Notes et Mémoires du Service Géologique du Maroc 315, p. 192.

Flecker, R., Krijgsman, W., Capella, W., de Castro Martíns, C., Dmitrieva, E., Mayser, J.P., Marzocchi, A., Modestou, S., Ochoa, D., Simon, D., Tulbure, M., van den Berg, B., van der Schee, M., de Lange, G., Ellam, R., Govers, R., Gutjahr, M., Hilgen, F., Kouwenhoven, T., Lofi, J., Meijer, P.T., Sierro, F.J., Bachiri, N., Barhoun, N., Alami, A.C., Chacon, B., Flores, J.A., Gregory, J., Howard, J., Lunt, D.J., Ochoa, M., Pancost, R., Vincent, S., Yousfi, M.Z., 2015. Evolution of the Late Miocene Mediterranean–Atlantic gateways and their impact on regional and global environmental change. Earth Sci. Rev. 150, 365–392.

Flores, J.A., Sierro, F.J., 1989. Calcareous nannoflora and planktonic foraminifera in the Tortonian-Messinian boundary interval of East Atlantic DSDP sites and their relation to Spanish and Moroccan section. In: Crux, J.A., van Heck, S.E. (Eds.), Nannofossils and Their applications. British Micropaleontological Society Series, pp. 249–266.

Foresi, L.M., et al., 2002. Calcareous plankton high resolution biostratigraphy (foraminifera and nannofossils) of the uppermost langhian–lower serravallianras il-pellegrin section (MALTA). Riv. Ital. Paleontol. Stratigr. 108 (2).

Frizon de Lamotte, D., 1979. Contribution à l'étude de l'évolution structural du Rif oriental (Maroc). (PhD thesis). Université Paris 6, France.

Frizon de Lamotte, D., 1981. L'olistostrome tortonien du Nékor et le problème de l'origine du matériel allochtone du Rif externe. Bull. Soc. Geol. Fr. 4, 419–427.

Gelati, R., Moratti, G., Papani, G., 2000. The Late Cenozoic sedimentary succession of the Taza-Guercif Basin, South Rifian Corridor, Morocco. Mar. Pet. Geol. 17, 373–390.

Goineau, A., Fontanier, C., Mojtahid, M., Fanget, A.-S., Bassetti, M.-A., Berné, S., Jorissen, F., 2015. Live–dead comparison of benthic foraminiferal faunas from the Rhône prodelta (Gulf of Lions, NW Mediterranean): development of a proxy for palaeoenvironmental reconstructions. Mar. Micropaleontol. 119, 17–33.

Guillemin, M., Houzay, J.P., 1982. Le Neogene post-nappes et le Quaternaire du Rif nord-oriental (Maroc). Stratigraphie et tectonique des bassins de Melilla, du Kert, de Boudinar et du piedmont des Kebdana. Notes et Mémoires du Service Géologique du Maroc 314, pp. 7–238.

Hilgen, F.J., Krijgsman, W., 1999. Cyclostratigraphy and astrochronology of the Tripoli diatomite formation (pre-evaporite Messinian, Sicily, Italy). Terra Nova-Oxford 11 (1), 16–22.

Hilgen, F.J., Krijgsman, W., Langereis, C.G., Lourens, L.J., Santarelli, A., Zachariasse, W.J., 1995. Extending the astronomical (Polarity) time scale into the Miocene. Earth Planet. Sci. Lett. 136, 495–510.

Hilgen, F.J., Bissoli, L., Iaccarino, S., Krijgsman, W., Meijer, R., Negri, A., Villa, G., 2000a. Integrated stratigraphy and astrochronology of the Messinian GSSP at Oued Akrech (Atlantic Morocco). Earth Planet. Sci. Lett. 182, 237–251.

Hilgen, F.J., Krijgsman, W., Raffi, I., Turco, E., Zachariasse, W.J., 2000b. Integrated stratigraphy and astronomical calibration of the Serravallian/Tortonian boundary section at Monte Gibliscemi (Sicily, Italy). Mar. Micropaleontol. 38 (3), 181–211.

Hüsing, S.K., Kuiper, K.F., Link, W., Hilgen, F.J., Krijgsman, W., 2009. The upper Tortonian–lower Messinian at Monte dei Corvi (Northern Apennines, Italy): completing a Mediterranean reference section for the Tortonian stage. Earth Planet. Sci. Lett. 282 (1), 140–157.

Krijgsman, W., Meijer, P.T., 2008. Depositional environments of the Mediterranean "Lower Evaporites" of the Messinian salinity crisis: constraints from quantitative analyses. Mar. Geol. 253, 73–81.

Krijgsman, W., Hilgen, F.J., Langereis, C.G., Zachariasse, W.J., 1994. The age of the Tortonian/Messinian boundary. Earth Planet. Sci. Lett. 121, 533–547.

Krijgsman, W., Hilgen, F.J., Langereis, C.G., Santarelli, A., Zachariasse, W.J., 1995. Late Miocene magnetostratigraphy, biostratigraphy and cyclostratigraphy in the Mediterranean. Earth Planet. Sci. Lett. 136, 475–494.

Krijgsman, W., Hilgen, F.J., Negri, A., Wijbrans, J.R., Zachariasse, W.J., 1997. The Monte del Casino section (Northern Apennines, Italy): a potential Tortonian/Messinian boundary stratotype? Palaeogeogr. Palaeoclimatol. Palaeoecol. 133, 27–47.

Krijgsman, W., Langereis, C.G., Zachariasse, W.J., Boccaletti, M., Moratti, G., Gelati, R., Iaccarino, S., Papani, G., Villa, G., 1999. Late Neogene evolution of the Taza-Guercif Basin (Rifian Corridor, Morocco) and implications for the Messinian salinity crisis. Mar. Geol. 153, 147–160.

Krijgsman, W., Blanc-Valleron, M.-M., Flecker, R., Hilgen, F.J., Kouwenhoven, T.J., Merle, D., Orszag-Sperber, F., Rouchy, J.-M., 2002. The onset of the Messinian salinity crisis in the Eastern Mediterranean (Pissouri Basin, Cyprus). Earth Planet. Sci. Lett. 194, 299–310.

Krijgsman, W., Gaboardi, S., Hilgen, F.J., Iaccarino, S., de Kaenel, E., van der Laan, E., 2004. Revised astrochronology for the Ain el Beida section (Atlantic Morocco): no glacio-eustatic control for the onset of the Messinian Salinity Crisis. Stratigraphy 1, 86–102.

Langereis, C.G., Zachariasse, W.J., Zijderveld, J.D.A., 1984. Late Miocene magnetobiostratigraphy of Crete. Mar. Micropaleontol. 8, 261–281.

Lourens, L., Hilgen, F.J., Laskar, J., Shackleton, N.J., Wilson, D., 2004. The Neogene Period. In: Gradstein, F., Ogg, J., Smith, A. (Eds.), A Geologic Time Scale. Cambridge University Press, London, pp. 409–440.

Martín, J.M., Braga, J.C., Betzler, C., 2001. The Messinian Guadalhorce corridor: the last northern, Atlantic-Mediterranean gateway. Terra Nova 13, 418–424.

Martín, J.M., Puga-Bernabéu, Á., Aguirre, J., Braga, J.C., 2014. Miocene Atlantic–Mediterranean seaways in the Betic Cordillera (southern Spain). Rev. Soc. Geol. Esp. 27, 175–186.

Martínez-García, P., Comas, M., Soto, J., Lonergan, L., Watts, A., 2013. Strike-slip tectonics and basin inversion in the Western Mediterranean: the post-Messinian evolution of the Alboran Sea. Basin Res. 26, 361–387.

Meijer, P.T., 2012. Hydraulic theory of sea straits applied to the onset of the Messinian Salinity Crisis. Mar. Geol. 326, 131–139.

Morel, J.L., 1989. Etats de contrainte et cinématique de la chaine Rifaine (Maroc) du Tortonien à l'actuel. Geodin. Acta 3, 238–294.
Mutti, E., Tinterri, R., Benevelli, G., di Biase, D., Cavanna, G., 2003. Deltaic, mixed and turbidite sedimentation of ancient foreland basins. Mar. Pet. Geol. 20, 733–755.
Pérez-Asensio, J.N., Aguirre, J., Schmiedl, G., Civis, J., 2012. Messinian paleoenvironmental evolution in the lower Guadalquivir Basin (SW Spain) based on benthic foraminifera. Palaeogeogr. Palaeoclimatol. Palaeoecol. 326, 135–151.
Platt, J.P., Allerton, S., Kirker, A., Mandeville, C., Mayfield, A., Platzman, E.S., Rimi, A., 2003. The ultimate arc: differential displacement, oroclinal bending, and vertical axis rotation in the External Betic-Rif arc. Tectonics 22, 1017.
Platt, J.P., Behr, W.M., Johanesen, K., Williams, J.R., 2013. The Betic-Rif arc and its orogenic hinterland: a review. Annu. Rev. Earth Planet. Sci. 41, 313–357.
Prosser, S., 1993. Rift-related linked depositional systems and their seismic expression. Geol. Soc. Lond., Spec. Publ. 71, 35–66.
Raffi, I., Flores, J.A., 1995. Pleistocene Trough Miocene Calcareous Nannofossils From Eastern Equatorial Pacific Ocean (ODP Leg 138). Scientific Results ODP, 138. Texas A&M University, pp. 233–286.
Raffi, I., Backman, J., Fornaciari, E., Pälike, H., Rio, D., Lourens, L., Hilgen, F.J., 2006. A review of calcareous nannofossils astrobiochronology encompassing the past 25 million years. Quat. Sci. Rev. 25:3113–3137. http://dx.doi.org/10.1016/j.quascirev.2006.07.007.
Reading, H.G., Collinson, J.D., 1996. Clastic coasts. In: Reading, H. (Ed.), Sedimentary Environments: Processes, Facies and Stratigraphy, 3rd ed Wiley-Blackwell, pp. 154–231.
Rogerson, M., Schönfeld, J., Leng, M.L., 2011. Qualitative and quantitative approaches in palaeohydrography: a case study from core-top parameters in the Gulf of Cadiz. Mar. Geol. 280, 150–167.
Romagny, A., Münch, Ph., Cornée, J.-J., Corsini, M., Azdimousa, A., Melinte-Dobrinescu, M.C., Drinia, H., Bonno, M., Arnaud, N., Monié, P., Quillévéré, F., Ben Moussa, A., 2014. Late Miocene to present-day exhumation and uplift of the Internal Zone of the Rif chain: insights from low temperature thermochronometry and basin analysis. J. Geodyn. 77, 39–55.
Roveri, M., Flecker, R., Krijgsman, W., Lofi, J., Lugli, S., Manzi, V., Sierro, F.J., Bertini, A., Carnerlenghi, A., De Lange, G., Govers, R., Hilgen, F.J., Huebscher, C., Meijer, P.T., Stoica, M., 2014. The Messinian Salinity Crisis: past and future of a great challenge for marine sciences. Mar. Geol. 352, 25–58.
Samaka, F., Benyaich, A., Dakki, M., Hcaine, M., Bally, A.W., 1997. Origine et inversion des bassins miocènes supra-nappes du Rif central (Maroc). Etude de surfaces et de subsurface. Exemple des bassins de Taounate et de Tafrant. Geodin. Acta 10, 30–40.
Sani, F., Del Ventisette, C., Montanari, D., Bendkik, A., Chenakeb, M., 2007. Structural evolution of the Rides Prerifaines (Morocco): structural and seismic interpretation and analogue modelling experiments. Int. J. Earth Sci. 96, 685–706.
Schönfeld, J., 1997. The impact of the Mediterranean Outflow Water (MOW) on benthic foraminiferal assemblages and surface sediments at the southern Portuguese continental margin. Mar. Micropaleontol. 29, 211–236.
Schönfeld, J., 2002. Recent benthic foraminiferal assemblages in deep high-energy environments from the Gulf of Cadiz (Spain). Mar. Micropaleontol. 44, 141–162.
Sierro, F.J., 1985. The replacement of the "*Globorotalia menardii*" group by the *Globorotalia miotumida* group: an aid to recognizing the Tortonian/Messinian boundary in the Mediterranean and adjacent Atlantic. Mar. Micropaleontol. 9, 525–535.
Sierro, F.J., Flores, J.A., Civis, J., González-Delgado, J.A., Frances, G., 1993. Late Miocene Globorotaliid event-stratigraphy and biogeography in the Ne-Atlantic and Mediterranean. Mar. Micropaleontol. 21, 143–168.
Sierro, F.J., Hilgen, F.J., Krijgsman, W., Flores, J.A., 2001. The Abad composite (SE Spain): a Messinian reference section for the Mediterranean and the APTS. Palaeogeogr. Palaeoclimatol. Palaeoecol. 168 (1), 141–169.
Simon, D., Meijer, P.T., 2015. Dimensions of the Atlantic–Mediterranean connection that caused the Messinian Salinity Crisis. Mar. Geol. 364, 53–64.
Sprovieri, M., Bellanca, A., Neri, R., Mazzola, S., Bonanno, A., Patti, B., Sorgente, R., 1999. Astronomical calibration of late Miocene stratigraphic events and analysis of precessionally driven paleoceanographic changes in the Mediterranean basin. Mem. Soc. Geol. Ital. 54, 7–24.
Suter, G., 1961. Carte Géologique du Rif, Feuille Rhafsai-Kelaa des Sles, échelle 1:50.000. Notes et Mémoires du Service Géologique du Maroc 164.
Suter, G., 1980. Carte géologique de la Chaine Rifaine, échelle 1:500.000. Ministère de l'Energie et des Mines du Maroc, Direction de la Géologie, Rabat. Notes et Mémoires du Service Géologique du Maroc 245a.
Suter, G., Mattauer, M., 1964. Carte Géologique du Rif, Feuille Taounate-Ain Aicha, échelle 1:50.000. Notes et Mémoires du Service Géologique du Maroc 166.
Tejera de Leon, J., Boutakiout, M., Ammar, A., Aït Brahim, L., El Hatimi, N., 1995. Les bassins du Rif central (Maroc): marqueurs de chevauchements hors sequence d'age Miocene terminal au coeur de la chaine. Bull. Soc. Geol. Fr. 166, 437–460.
Topper, R.P.M., Flecker, R., Meijer, P.T., Wortel, M.J.R., 2011. A box model of the Late Miocene Mediterranean Sea: implications from combined $^{87}Sr/^{86}Sr$ and salinity data. Paleoceanography 26, PA3223.
Turco, E., Bambini, A.M., Foresi, L., Iaccarino, S., Lirer, F., Mazzei, R., Salvatorini, G., 2002. Middle Miocene high-resolution calcareous plankton biostratigraphy at Site 926 (Leg 154, equatorial Atlantic Ocean): palaeoecological and palaeobiogeographical implications. Geobios 35, 257–276.
Van Assen, E., Kuiper, K.F., Barhoun, N., Krijgsman, W., Sierro, F.J., 2006. Messinian astrochronology of the Melilla Basin: stepwise restriction of the Mediterranean–Atlantic connection through Morocco. Palaeogeogr. Palaeoclimatol. Palaeoecol. 238, 15–31.
Van den Berg, B.C.J., 2016. Improved Biostratigraphic Dating of Upper Miocene Sediments in Western Betics Suggests Late Tortonian Closure of the Guadalhorce Corridor. Chapter 4, pp. 125–135 in PhD thesis: Late Miocene Astrochronology and Basin Evolution of the Atlantic Side of the Betic Corridor Linked to the Messinian Salinity Crisis. Salamanca University, Salamanca, Spain.
Van den Berg, B.C.J., Sierro, F.J., Hilgen, F.J., Flecker, R., Larrasoaña, J.C., Krijgsman, W., Flores, J.A., Mata, M.P., Martín, E.B., Civis, J., González-Delgado, J.A., 2016. Astronomical tuning for the upper Messinian Spanish Atlantic margin: disentangling basin evolution, climate cyclicity and MOW. Glob. Planet. Chang. 135, 89–103.
Van den Berg, B.C., Sierro, F.J., Hilgen, F.J., Flecker, R., Larrasoaña, J.C., Krijgsman, W., Flores, J.A., Mata, M.P., 2017. Imprint of Messinian Salinity Crisis events on the Spanish Atlantic margin. Newsl. Stratigr.
Van der Schee, M., 2016. Mediterranean-Atlantic Water Exchange Over the Miocene-Pliocene Boundary. (PhD thesis). Universidad de Salamanca, Spain.
Van Hinsbergen, D.J.J., Vissers, R.L.M., Spakman, W., 2014. Origin and consequences of western Mediterranean subduction, rollback, and slab segmentation. Tectonics 33, 393–419.
Vergés, J., Fernàndez, M., 2012. Tethys–Atlantic interaction along the Iberia–Africa plate boundary: the Betic–Rif orogenic system. Tectonophysics 579, 144–172.
Vidal, J.C., 1979. Carte Géologique du Maroc, Feuille Dhar Souk, échelle 1:50.000. Notes et Mémoires du Service Géologique du Maroc 298.
Wernli, R., 1977. Les foraminifères planctoniques de la limite mio-pliocène dans les environs de Rabat (Maroc). Eclogae Geol. Helv. 70, 143–191.
Wernli, R., 1988. Micropaléontologie du Néogène post-nappes du Maroc septentrional et description systématique des foraminifères planctoniques. Notes et Mémoires du Service Géologique du Maroc 331 (266 pp).
Wildi, W., 1983. La chaîne tello-rifaine (Algérie, Maroc, Tunisie): structure, stratigraphie et évolution du Trias au Miocène. Rev. Géol. Dynam. Géog. Phys. 24, 201–297.
Young, J., Flores, J.A., Wei, W., 1994. A summary chart of Neogene Nannofossils magnetobiostratigraphy. Journal of Nannoplankton Research 16 (1), 21–27.
Young, J.R., Bown, P.R., Lees, J.A. (Eds.), 2014. Nannotax3 Website. International Nannoplankton Association (URL: http://ina.tmsoc.org/Nannotax3; 21 Apr.).
Zachariasse, W.J., 1975. Planktonic foraminiferal biozonation of the Late Neogene of Crete (Greece). Utrecht Micropaleontol. Bull. 11 (171 pp).
Zizi, M., 1996. Triassic–Jurassic extension and Alpine inversion in the northern Morocco. In: Ziegler, P.A., Horvath, F. (Eds.), Peri-Tethys Memoir 2: Structure and Prospects of the Alpine Basins and Forelands. Mémoires du Muséum National d'Histoire Naturelle 170, pp. 87–101 Paris.